Leisure Boat Design: A Comprehensive Study of the Shape and Dimension Effects on Hydrodynamic Performances

Naufal Nur Saifullah
Department of Mechanical Engineering, Universitas Sebelas Maret

Aditya Rio Prabowo
Department of Mechanical Engineering, Universitas Sebelas Maret

Muhayat, Nurul
Department of Mechanical Engineering, Universitas Sebelas Maret

Tuswan Tuswan
Department of Naval Architecture, Universitas Diponegoro

他

https://doi.org/10.5109/7236854

出版情報：Evergreen. 11 (3), pp.2091-2119, 2024-09. 九州大学グリーンテクノロジー研究教育センター
バージョン：

Leisure Boat Design: A Comprehensive Study of the Shape and Dimension Effects on Hydrodynamic Performances

Naufal Nur Saifullah[1], Aditya Rio Prabowo[1,*], Nurul Muhayat[1], Tuswan Tuswan[2], Catur Harsito[3], Ristiyanto Adiputra[4], Martin Jurkovič[5], Seung Jun Baek[6]

[1]Department of Mechanical Engineering, Universitas Sebelas Maret, Surakarta, 57126, Indonesia

[2]Department of Naval Architecture, Universitas Diponegoro, Semarang 50275, Indonesia

[3]Department of Mechanical Engineering, Vocational School, Universitas Sebelas Maret, Surakarta, 57126, Indonesia

[4]Research Center for Hydrodynamics Technology, National Research and Innovation Agency, BRIN, Surabaya, 60112, Indonesia

[5]Faculty of Operation and Economics of Transport and Communication, University of Zilina, Zilina 01026, Slovakia

[6]Advanced-Green Technology Center, Korea Marine Equipment Research Institute, Busan, 46744, South Korea

*Author to whom correspondence should be addressed:
E-mail: aditya@ft.uns.ac.id

(Received October 28, 2023: Revised May 25, 2024: Accepted June 21, 2024).

Abstract: Marine tourism has been essential in the tourism industry for many years. The marine tourism sector plays an essential role in the Indonesian economy. An example of the marine tourism industry is in the Lombok islands, West Nusa Tenggara. The role of ships as a means of transportation and recreation is vital in the marine tourism industry. However, there are still many uses for ships with traditional hulls that need better hydrodynamic performance. Therefore, it is necessary to research the hull model of recreational ships (leisure boats) to improve hydrodynamic performance so that the role of ships as a means of recreation and transportation can make passengers and tourists safer and more comfortable. This study discusses the influence of hull dimensions and shape variations on hydrodynamic performance using five reference vessels with Length Over All (LOA) of 9-10 m. Regression analysis methods are carried out to produce three-dimensional variations and combine four types of hulls: Shallow V, Deep V, Round Hull, and Flat Bottom Hull. The dimension and shape variation will result in twelve model hull variations. Each model is simulated and analyzed for hydrodynamic performance using sensitivity analysis to determine the influence of variations in hull dimensions and shape determination of the best model from twelve hull variations using the multi-attribute decision-making (MADM) method. The results of MADM found that the hull with the Shallow V model has the best hydrodynamic characteristics and dimensional variations in the hull shape significantly influence the ship's hydrodynamic performance. The results are expected to optimize the hydrodynamical performance of the Leisure Boat.

Keywords: Mono hull; leisure boat; hydrodynamic performance; design variation

1. Introduction

Marine tourism has played an important role in the tourism industry for many years. The Indonesian Ministry of Culture and Tourism states that marine tourism is a type of special interest tourism with activities with the marine, both above sea level and activities carried out at sea level. Marine tourism also significantly benefits land tourism, especially in coastal areas, and brings positive impacts and real economic increases, especially to coastal communities. The potential of marine tourism in Indonesia is very large, but it only contributes a relatively small amount. Marine tourism only contributed US $ 3.5 billion to the gross domestic product (GDP) in 2013. The Indonesian government in 2019 targeted 4 million contributions of local and international visitors from this marine tourism[1)]. Projections of marine tourism in 2015 can be seen in the pie chart in Fig. 1[2)].

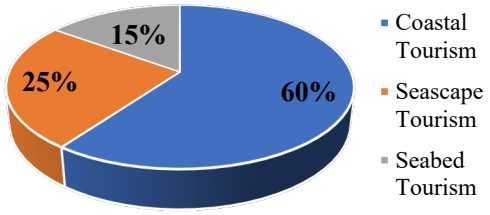

Fig. 1: Projections of marine tourism in Indonesia in 2015.

One of the contributors to marine tourism in Indonesia is Lombok. Lombok is one of the islands in West Nusa Tenggara Province, separated by the Lombok Strait from Bali and the Alas Strait to the east of Sumbawa. Marine tourism that can be done in Lombok is divided into three types: coastal zone, marine zone, and sub-marine zone. In coastal tourism, the types of activities can be done, namely playing sand, picnics, and sunbathing. Furthermore, in seascape tourism, the activities that can be done are yachting, cruising, and surfing. Then, on seabed tourism, diving and snorkeling can be performed[3]. The condition of the Lombok islands for marine tourism is shown in Fig. 2. One of the efforts to advance recreational infrastructure for marine tourism in Lombok is to develop a hull model with stability and good ship movement so that tourists are more comfortable when travelling, thus increasing the interest of local and foreign tourists.

Fig. 2: Marine tourism areas in Lombok islands.

This study aims to determine the influence of hull shape and variation of hull dimensions on the hydrodynamic characteristics of the hull[4]. In this study, regression methods were analyzed to determine the dimensions of the main size of the vessel. The regression method analysis was chosen because it can get a measure with a similarity of 99.474% with its reference[5]. Variations in the dimensions of different hull sizes and shapes result in diverse performance of resistance, stability, seakeeping, Motion Sickness Incidence (MSI), slamming, and deck wetness. Simulations on variations of hull models carried out in this study are resistance, stability, seakeeping, MSI, slamming, and deck wetness using Maxsurf software. Savitsky and Holtrop's methods are used for resistance analysis, large angle stability is used for stability analysis on ships, and strip theory is used for seakeeping, MSI, slamming, and deck wetness analysis. Sensitivity analysis is used to determine variations in hull shape and hull dimension variations that affect the ship's hydrodynamic performance according to the leisure boat's needs[6]. Furthermore, it compares the test results between variations of hull models using MADM method to calculate the ranking based on overall simulation results[7].

2. Theoretical Method

2.1 Regression Method

In designing a hull shape, the main size of the ship is needed. The main size of the ship is obtained from the regression results[8]. Regression analysis is a modelling approach that uses an approach from 1 variable to another. Generally, the variables X (independent variable) and Y (dependent) are used. Variable X is an independent or causal variable, while variable Y is a result or effect variable. In this study, regression analysis was used in determining the main size of the ship using the relationship of ship length data (LOA), ship width (B), ship height (D), and ship weight (Δ)[9]. The regression analysis method carried out in this study is linear regression. Linear regression is a modelling approach that uses the relationship of ship main data (LOA, B, D, Δ) by following a straight line. The mathematical model for linear regression is shown in Eq. 1.

$$Y = aX + b \tag{1}$$

where Y and X are variable, while a and b are constant.

2.2 Ship Resistance

Ship resistance is one of the hydrodynamic performance parameters of the hull. In designing ships, predicting resistance values is important[10]. Ship resistance has several types, including friction, wave generation, and hull shape drag[11,12]. When the ship operates, several factors affect ship speed (Vs), ship weight, and ship shape[13]. The total resistance of the ship can be seen in Eq. 2.

$$R_T = R_F + R_{pv} + R_w \tag{2}$$

where R_T is the total resistance, R_{pv} is the viscous pressure resistance, and R_w is the wave resistance.

2.2.1 Savitsky Method

When planning speed circumstances, the Savitsky method is a numerical technique used in hydrodynamic computations to find the ship's resistance, wetted surface, center of pressure, and hull drag. In addition, the Savitsky

method can set speed, trim, deadrise angle, and load parameters[14]. The Savitsky method assumes that the planning hull is in a steady-state condition, implying no acceleration in any direction[15,16]. Therefore, the formula in the study is based on the Savitsky method. The formulas used in Savitsky method can be seen in Eqs. 3 and 4.

$$D_f = \frac{c_f \rho V_1^2 (\lambda b^2)}{2 \cos \beta} \quad (3)$$

$$D = \Delta \tan \tau + \frac{D_f}{\cos \tau} \quad (4)$$

where D_f is the frictional resistance, λ is the average value of the ratio of length and width in the wet area, b is the mean chine beam of planing craft, β is the deadrise angle of planning hull, D is the total drag, Δ is total displacement force, and τ is the trim angle of planning hull.

2.2.2 Holtrop Method

The Holtrop method is a method for determining the resistance and power of a displacement-type ship's hull[17]. This method is appropriate to use if the parameters used follow modelling. Therefore, expansion is carried out using the L/B ratio, adjusting the submerged transom stem. The prediction formula is presented in Eq. 5 for the hull form factor[18].

$$1 + k_1 = c_{13}\left\{0.93 + c_{12}\left({}^{B}/_{L_R}\right)^{0.92497}(0.95 - C_p)^{-0.521448}(1 - C_p + 0.0255\, lcb)^{0.6906}\right\} \quad (5)$$

Eq. 6 shows the determination of the addition of resistance.

$$R_{APP} = 0.5\, \rho . V^2 S_{APP} (1 + K_2)_{eq} C_f \quad (6)$$

where ρ is the water density, V is the ship speed, S_{APP} is the wetted area of the appendage, $1 + K_2$ is the resistance factor of the appendage, and C_f is the frictional resistance coefficient of the ship according to the ITTC-1957 formula.

2.3 Ship Stability

Ship stability is the ability of a ship to return to its initial position when receiving external forces[19,20]. Some important ship stability factors are buoyancy, gravity, and metacentric points[21]. The points that affect the ship's stability can be seen in Fig. 3.

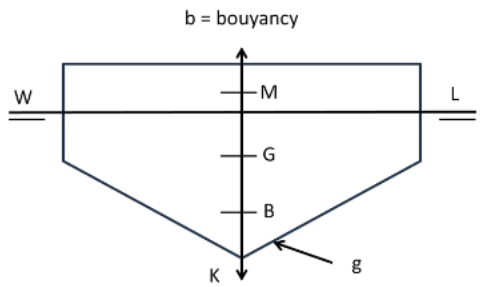

Fig. 3: Stability point on a ship.

The ship will experience shock when external forces occur. The shock will transform the ship's center of buoyancy. Changes in the angle of inclination of the ship will result in the force received by the ship and affect the value of the righting lever curve (GZ). The righting lever (GZ) curve is used to determine the safety level of the ship. Based on regulations from the International Maritime Organization (IMO). The stability reference criteria based on IMO HSC200 Section A.749 are as follows[22]:

- The area under the GZ curve up to an angle of 30° is not less than 0.055 m.rad or 3.151 m.deg.
- The area under the GZ curve up to an angle of 40° is not less than 0.09 m.rad or 5.517 m.deg.
- The area under the GZ curve between an angle of 30° and 40° is not less than 0.03 m.rad or 1.719 m.deg.
- The GZ arm at heel angles equal to or greater than 30° shall not be less than 0.2 m.
- The maximum GZ arm shall occur at a heel angle of not less than 25°.
- Initial metacenter points height GM_0 not less than 0.15 m.

2.4 Seakeeping Analysis

Ship seakeeping analysis is very important because it greatly affects the ship's performance in habitability, usability, and safety[23]. he seakeeping ability of ships is used to determine ship performance in various water conditions. Seakeeping analysis consists of three motions: heaving, rolling, and pitching[24]. When the ship encounters waves, the ship will move following six axes, encompassing heave, pitch, yaw, sway, surge, and roll, as seen in Fig. 4.

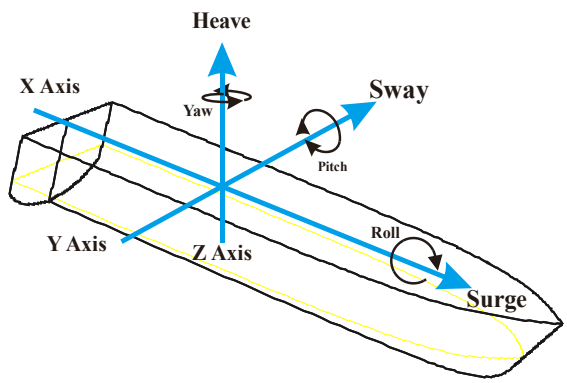

Fig. 4: Six degrees of freedom on ship's hull.

2.4.1 Heaving

Heaving is an up-downwards movement parallel to the z-axis. To determine the value of heaving, one can use Eq. 7.

$$a\ddot{z} + b\dot{z} + cz = F_0 Cos\omega_\theta t \quad (7)$$

where $a\ddot{z}$ is the inertial force, $b\dot{z}$ is the damping force, cz is the restoring force, and $F_0 Cos\omega_\theta t$ is the exciting force.

2.4.2 Rolling

Rolling is rotating occurring due to wave action. This type of motion is frequently created by waves heading perpendicular to the ship's direction of motion. Roll movement analysis uses the following Eq. 8.

$$a\frac{d^2\emptyset}{dt} + a\frac{d\emptyset}{dt} + c\emptyset = M_o cos\omega_\theta t \quad (8)$$

where $a\frac{d^2\emptyset}{dt}$ is the inertial force, $a\frac{d\emptyset}{dt}$ is the damping force, $c\emptyset$ is the restoring force, and $M_o cos\omega_\theta t$ is the exciting force.

2.4.3 Pitching

Pitching is the rotating occurring about a transverse axis. This motion can occur because of waves that cause a height difference between a hull's front and back[25]. Eq. 9 is used to determine the pitching motion.

$$d\ddot{\emptyset} + e\emptyset + h\emptyset = M_{0.} Cos\omega_e t \quad (9)$$

where $d\ddot{\emptyset}$ is the inertial force, $e\emptyset$ is the damping force, $h\emptyset$ is restoring force, and $M_{0.}\mathrm{Cos}\omega_e\mathrm{t}$ is the exciting force.

2.4.4 RAO

The operator response amplitude (RAO) is a parameter for analysing a vessel's response to ocean wave movement or other disturbances. RAO measures the response or amplitude of a ship's motion in response to external forces. The RAO predicts forces on ships, such as surge, sway, heave, roll, pitch, and yaw[26,27]. The formula of RAO is shown explicitly in Eq. 10.

$$RAO = \left(\frac{\emptyset_a}{\zeta_a}\right)^2 \quad (10)$$

where $\emptyset_a$ is the ship motion response amplitude, and ζ_a is the incident wave amplitude (deg).

2.4.5 Motion Sickness Incidence (MSI)

MSI is one of the parameters of passenger comfort level when the ship sails. Motion sickness is characterized by unpleasant physical sensations such as dizziness, nausea, pallor, difficulty breathing, and vomiting[28]. It is commonly referred to as seasickness due to a ship's motion. The cause of seasickness, according to the International Standard reference (ISO 2631), is vertical acceleration. Table 1 below shows the comfort level of a ship based on vertical speed.

Table 1. Comfort level and vertical acceleration.

Habitability Acceleration (RMS) (m.s^{-2})	**Parameter**
< 0.315	Not Uncomfortable
0.315 – 0.63	A little Uncomfortable
0.5 – 1.0	Fairly Uncomfortable
0.8 – 1.6	Uncomfortable
-2.5	Very Uncomfortable
>2	Extremely Uncomfortable

The MSI index is used to determine the probability of seasickness. The following Eq. 11 is used to calculate the MSI index[29].

$$MSI = 100\left[0.5 + erf\left(\frac{log_{10}(0.798\sqrt{m_4}/g) - \mu_{MSI}}{0.4}\right)\right] \quad (11)$$

where m_4 is spectral moment of the ship and g is the gravity force.

2.4.5 Slamming and Deck Wetness

Slamming and deck wetness are undesirable occurrences when ships are operating. Both can cause structural damage to the ship's hull and impact the comfort of the ship's crew and passengers[30]. Deck wetness is the result of rising seawater on the ship's deck, which will create damage and impact the comfort of the crew and passengers of the ship. Deck wetness can occur due to extreme waves or forces on the ship. Meanwhile, slamming on ships occurs when the bottom of the hull meets the water's surface at high speed, causing great pressure on the hull. Slamming can damage the hull and have a major impact on the ship's balance. The formula for calculating deck wetness and slamming values is shown in Eqs. 12 and 13[29].

$$P(Deck\ wetness) = exp\left(\frac{-fe^2}{2m_0}\right) \quad (12)$$

$$P(slamming) = exp\left(-\frac{d^2}{2m_0} - \frac{Vcr^2}{2m_2}\right) \quad (13)$$

where m_0 is the relative vertical motion spectrum, fe is the effective board, m_2 is the relative vertical velocity spectrum, Vcr is the threshold velocity, and d is the draft.

2.5 Sensitivity Analysis

In this study, sensitivity analysis was carried out to determine the effect of each variation to be tested. In this

study, variable variations are created in input values and impact the output values that have been measured. This sensitivity analysis aims to determine how much influence each input variable has on the output variable in helping decision-making and strategic planning.

Estimation of the results of a parameter is considered sensitive if there is a change in a parameter that causes drastic changes in value. Conversely, the estimated results obtained do not change in value. So, the estimation results are relatively insensitive to the value of these parameters[31]. In conducting sensitivity analysis, it should be noted that results may vary depending on the model or system used and the range of values selected for each variable. This sensitivity analysis is expected to make good decisions in the design process to optimize ship design following the desired performance goals.

2.6 Multi-Attribute Decision Making (MADM)

MADM is based on several attributes or related alternative criteria[32]. The simple weighted addition method (SAW) is a type of MADM method used for simple weighting. The easy SAW method makes it popular in the practitioner environment[33]. Finding the total of the performance rating weightings for each alternative of all qualities is the basic idea behind the SAW approach. For the SAW approach to scale and compare with all alternative ratings, the decision matrix x must be normalized. Eq. 14 defines how to normalize the decision matrix. After that, Eq. 15 is used to determine the preference value of each option.

$$r_{ij} = \begin{cases} \dfrac{x_{ij}}{Max_i x_{ij}} & Maximum\ Criteria\ Value \\ \dfrac{Min_i x_{ij}}{x_{ij}} & Minimum\ Criteria\ Value \end{cases} \quad (14)$$

$$V_i = \sum_{j=1}^{n} w_i r_{ij} \quad (15)$$

Where V_i is the preference value, w is the weight of the criteria, and r is the normalized alternative value.

2.7 Monohull Shape Type

Ships with monohull types consist of several hull variations that adjust as needed. Hull shape can significantly affect a ship's wave flow patterns and hydrodynamic performance characteristics. Each type of hull has its uses, advantages, and weaknesses. The choice of hull shape is critical for optimizing comfort and enhancing the tourist experience in the waters around Lombok Island. Therefore, this research uses four monohull form types such as Shallow V, Deep V, Round Bottom, and Flat Bottom.

The shallow V hull is one type of planning hull. The shape is like the letter v from the back view and has two edges below where there is a space in the middle between the left and right surfaces. The shallow V hull type is usually used for patrol boats, rescue ships, ambulance ships, offshore supply ships, leisure ships, and sports competitions[34,35]. The Shallow V hull was chosen for leisure boat because it is ideal for operating in moderate to slightly choppy waters.

The deep v hull variations have a shape similar to shallow v, but deep v has a higher deadrise angle (20 deg.)[36]. Deep V Hull is typically employed in fast boats due to its ability to reduce resistance and provide a smoother ride in rough waters, making it a suitable choice for high-speed leisure boat.

The round bottom hull has a semi-circle-like shape with a curved or concave bottom. The round bottom hull is a displacement hull type that prioritizes buoyancy[37]. The round bottom hull is used on cargo ships and ships sailing at low speed. The round bottom hull was chosen for leisure boat because its ability to glide smoothly on the water and reduce resistance when moving.

The flat bottom hull has a flat shape at the bottom. A flat bottom hull is a displacement hull type that prioritizes buoyancy. The flat bottom hulls are used on cargo ships, surveillance ships, and ships at low speeds. The flat bottom hull was chosen for leisure boat because it is optimal for operating in shallow waters. An illustration of the variation of the monohull shape type is shown in Fig. 5.

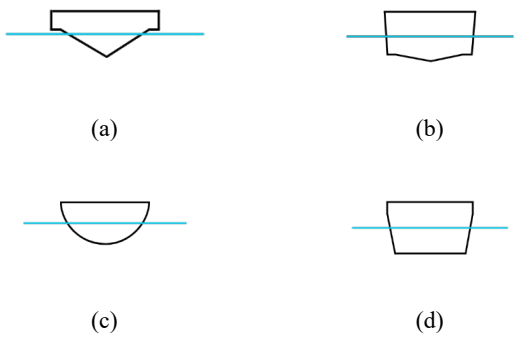

Fig. 5: Monohull-type variations: (a) Deep V; (b) Shallow V; (c) Round Bottom; (d) Flat Bottom.

3. Research Method

3.1 Ship References

In this study, the reference vessel's size was obtained with the parameters of LOA 9-10 m with the main sizes including LOA, Beam, Depth, Draft, and DWT (Δ). Data on the main sizes of ships can be seen in Table 2.

Table 2. Reference ship data.

No	Reference Ships	Δ (ton)	LOA (m)	B (m)	H (m)	T (m)
1	Chaparral 300 OSX	3.85	9.91	2.9	1.45	0.56
2	Galeon 325 GTO	5.89	9.93	3.24	1.64	0.86
3	Beneteau Antares 11	6.1	9.9	3.51	1.75	0.71
4	Cap Camarat 9.0 WA	2.48	9.12	2.98	1.49	0.63
5	Pursuit S288 Sport	3.72	9.14	2.95	1.47	0.91

3.2 Regression Variations

After obtaining five reference vessels, the main size data of the new leisure vessels can be determined using linear regression approach analysis. This study uses displacement as an independent variable. The results chart of the regression for the five reference vessels can be seen in Fig. 6.

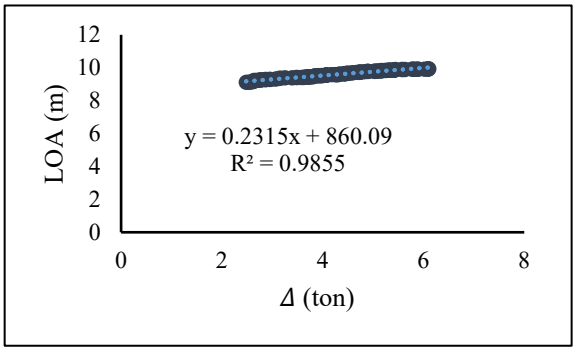

(a)

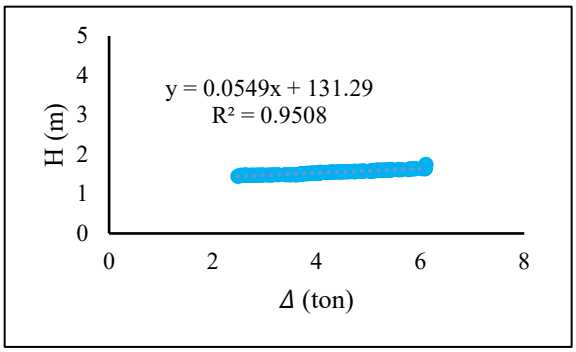

(b)

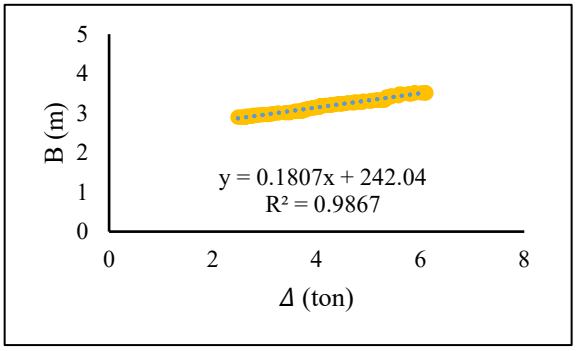

(c)

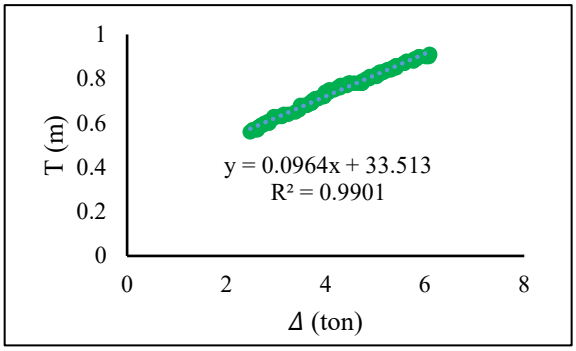

(d)

Fig. 6: Regression result: (a) LOA vs. displacement; (b) depth vs. displacement; (c) beam vs. displacement; (d) draft vs. displacement.

Based on the results of linear regression, a linear equation is used to create dependent variables. This research used a target displacement of 4.40 tons taken from the average displacement of the five reference ships. Furthermore, calculations are performed to produce the value of y, and the displacement target is used as the value of x. The results of the primary dimensions calculation can be seen in Table 3.

Table 3. The dimensions of regression results.

Parameter	Value
LOA (m)	9.60
Beam (m)	3.12
Depth (m)	1.56
Draft (m)	0.73
Displacement (ton)	4.40

This study analyses the effect of hydrodynamic characteristics on hull dimension variations and hull shape variations. Therefore, it is very important to do regression again to obtain three-dimension variations. Three-dimension variations are obtained by locking three dependent variables: displacement with LOA, displacement with beam, and displacement with draft. The value of one of these three sets is a fixed variable, and the remaining value is a regression calculation. The results of the regression calculation to obtain the first variation dimension by locking the LOA with displacement can be seen in Fig. 7. The results of the second variation dimension regression calculation by locking the beam

with displacement are shown in Fig. 8. Furthermore, the results of the regression calculation of the third variation dimension by locking depth with displacement are shown in Fig. 9.

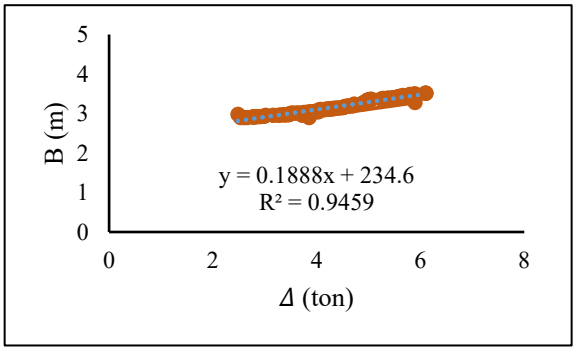

(a)

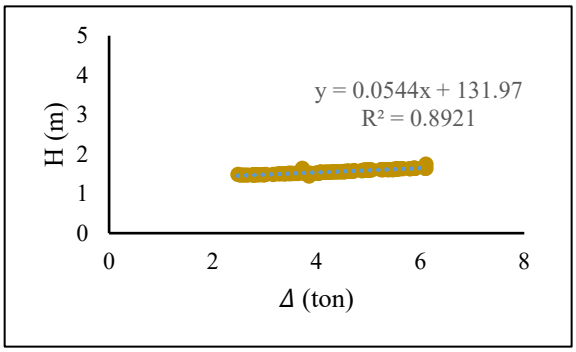

(b)

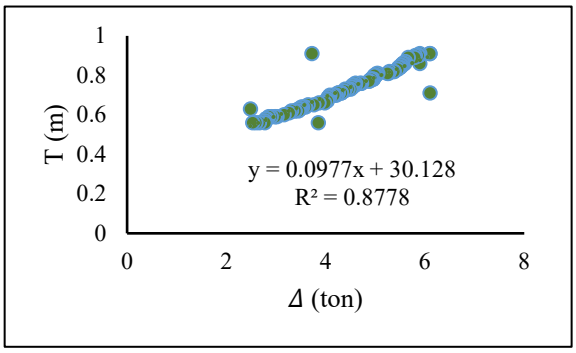

(c)

Fig 7: Regression result for Variation A with the locking of LOA with displacement: (a) beam vs. displacement; (b) depth vs. displacement; (c) draft vs. displacement.

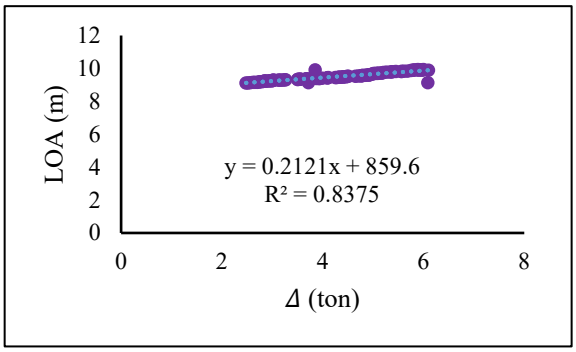

(a)

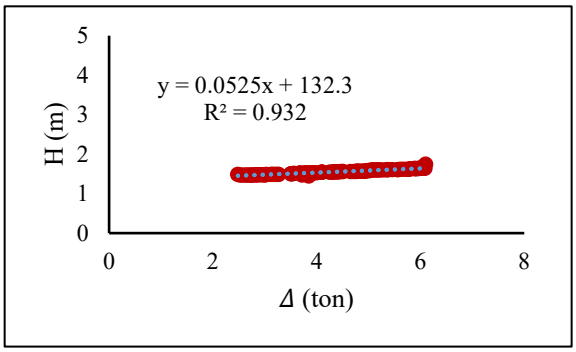

(b)

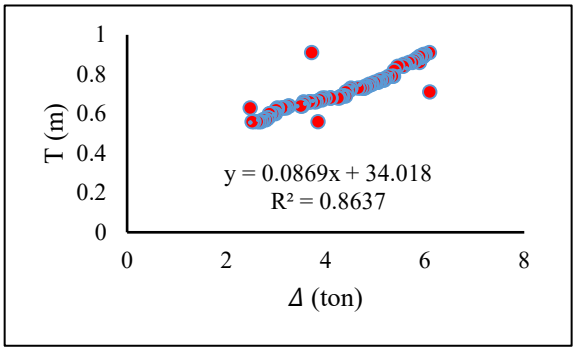

(c)

Fig. 8: Regression result for Variation B with the locking of beam with displacement: (a) LOA vs. displacement; (b) depth vs. displacement; (c) draft vs. displacement.

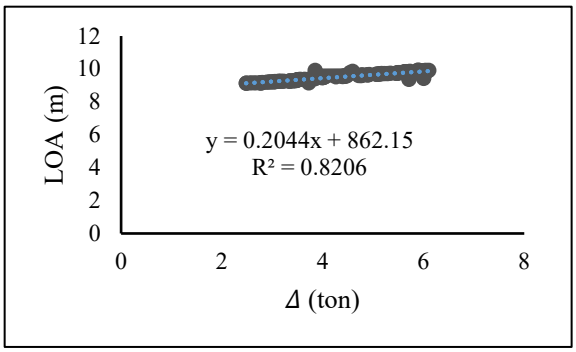

(a)

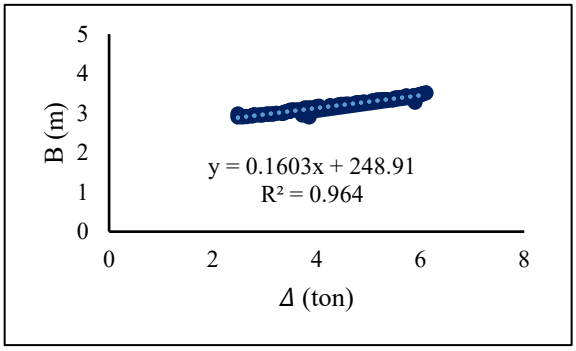

(b)

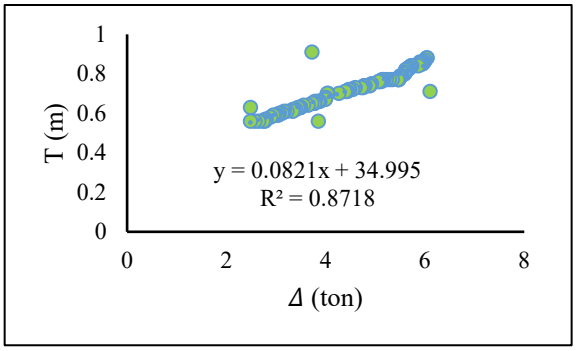

(c)

Fig. 9: Regression result for Variation C with the locking of depth with displacement: (a) LOA vs. displacement; (b) beam vs. displacement; (c) draft vs. displacement.

The result of regression calculations produces three-dimensional variations. The first variation is the result of locking LOA with displacement data, the second is the result of locking beam with displacement, and the third is the result of locking depth with displacement. The recapitulation of dimension variation using the regression method is shown in Table 4.

Table 4. Recapitulation of the dimension variations using regression method.

Parameter	Value		
	Variation 1	**Variation 2**	**Variation 3**
LOA (m)	9.62	9.52	9.53
B (m)	3.21	3.17	3.20
H (m)	1.55	1.56	1.55
T(m)	2.48	9.12	2.98
Δ (ton)	4.40	4.40	4.40

After obtaining the ship dimension data, the next step is to do the 3D Hull modelling for each variation with four hull shapes (Deep V Hull, Shallow V Hull, Flat Bottom Hull, and Round Hull). This test resulted in twelve hull variations that will be analyzed for the effect of hull shape on hydrodynamic performance character. The 3D models with variations in hull shape, as shown in Fig. 10.

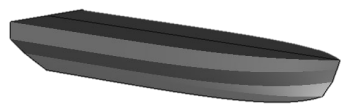

(a)

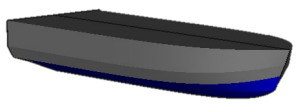

(b)

(c)

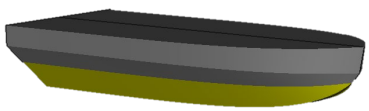

(d)

Fig. 10: Isometric perspective model hull variation: (a) Deep V Hull; (b) Shallow V Hull; (c) Round Hull; (d) Flat Bottom Hull.

3.3 Simulation Analysis

After the three-dimensional design modelling process is complete, the next stage is to simulate twelve hull variations to evaluate the hydrodynamic attributes in each variation. A recapitulation of the model can be seen in Table 5.

Table 5. Model recapitulation.

Model	Δ (ton)	LOA (m)	B (m)	H(m)	T (m)
Deep V Hull A	4.40	9.62	3.21	1.55	0.76
Deep V Hull B	4.40	9.52	3.17	1.56	0.73
Deep V Hull C	4.40	9.53	3.20	1.55	0.72
Shallow V Hull A	4.40	9.62	3.21	1.55	0.76
Shallow V Hull B	4.40	9.52	3.17	1.56	0.73
Shallow V Hull C	4.40	9.53	3.20	1.55	0.72
Round Bottom Hull A	4.40	9.62	3.21	1.55	0.76
Round Bottom Hull B	4.40	9.52	3.17	1.56	0.73
Round Bottom Hull C	4.40	9.53	3.20	1.55	0.72
Flat Bottom Hull A	4.40	9.62	3.21	1.55	0.76
Flat Bottom Hull B	4.40	9.52	3.17	1.56	0.73
Flat Bottom Hull C	4.40	9.53	3.20	1.55	0.72

In this study, the influence of environmental factors was also considered[38], and simulations were carried out using parameters in the environmental conditions of the waters of Lombok, West Nusa Tenggara, Indonesia. This data is taken from sea temperature published online[39]. Water density data is taken from fresh water and seawater properties at the International Towing Tank Conference (ITTC) based on the water temperature conditions[40]. Environmental parameter factors can be seen in Table 6.

Table 6. Dimensions of regression results.

Parameter	Value	Unit
Water density	1022	kg/m^3
Windspeed	6	kts
Wave height	0.7	m

Resistance simulation is carried out using Savitsky method for Deep V and Shallow V simulation. The Holtrop method is used for the round bottom and flat bottom simulation. Resistance analysis is carried out with speed parameters of 0-50 kts, producing the resistance value and power value needed when the ship operates.

In stability simulation, Maxsurf Stability Software is used to analyze the stability ability of the ship. Stability simulation is done with a tilt angle of 0 deg. Until 180 deg. The method used is large angle stability with free trim load case setting. The results of the stability simulation produce a stability value when the ship is static with the value of the GZ arm.

Maxsurf Motions Software is used to simulate seakeeping using the strip theory method. The ship's hull is separated into 41 earlier pieces for investigation, although it is not in the mesh. In this study, wave directions of beam sea (90 deg.), bow quartering (135 deg.), and head sea (182 deg.) were studied using a sailing speed of 20 knots and an average wave height of 0.7 m on Lombok Island. JONSWAP spectra are the kind of wave spectra utilized in this investigation. The results of the seakeeping simulation are displayed with RAO charts in heaving, rolling, and pitching movement and also produced charts from MSI to determine the response of the ship's motion when hitting waves and the level of seasickness in the ship's passengers when sailing. In addition, seakeeping simulation also produces slamming values and deck wetness values on ships. In this study, the influence of the type of propulsion and hull construction was negligible[41].

4. Results and Discussion

4.1 Result of Resistance Simulation

Resistance analysis was carried out from twelve variations of ship hulls based on shape variation and dimension variation. The simulated results of resistance vs speed and power vs speed are shown in Tables 7 and 8, also shown in Figs. 11-18. The Wave Contour of the resistance simulation results are shown in Figs. 19-21.

Table 7. Resistance result of twelve ship variation.

Speed (kts)	Resistance (kN)											
	Hull Type											
	Deep V Hull			Shallow V Hull			Flat Bottom Hull			Round Hull		
	A	B	C	A	B	C	A	B	C	A	B	C
10	5.86	5.23	5.12	12.06	10.49	10.74	13.66	12.84	12.63	15.64	14.53	14.32
15	8.27	7.42	7.27	15.06	13.69	13.43	19.23	18.09	17.79	19.11	17.78	17.54
20	10.35	9.30	9.12	17.04	15.40	15.13	22.48	20.95	20.58	21.97	20.27	19.97
25	11.30	10.19	10.00	16.93	15.31	15.01	22.60	20.95	20.58	21.78	20.00	19.71
30	11.88	10.76	10.59	16.72	15.21	15.02	22.16	20.52	20.18	20.95	19.29	19.05
35	12.64	11.50	11.34	17.04	15.63	15.56	22.16	20.54	20.23	20.64	19.12	18.95
40	13.72	12.53	12.39	17.97	16.61	16.64	22.77	21.14	20.85	21.07	19.66	19.54
45	15.14	13.88	13.75	19.44	18.09	18.22	23.95	22.28	22.01	22.18	20.84	20.78
50	16.87	15.51	15.40	21.39	20.01	19.96	25.65	23.90	23.64	23.89	22.58	22.57

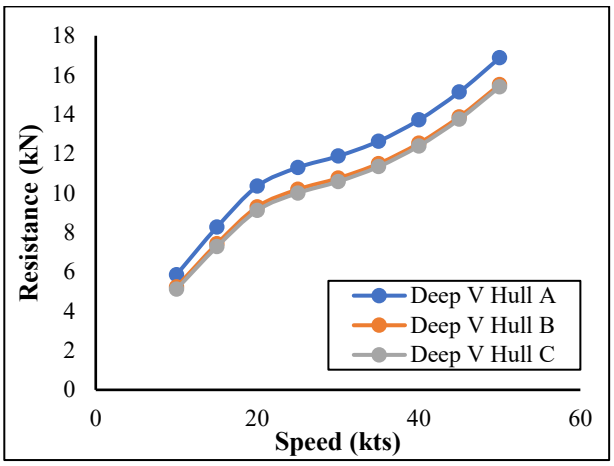

Fig. 11. Resistance vs. speed on the deep V hull variations.

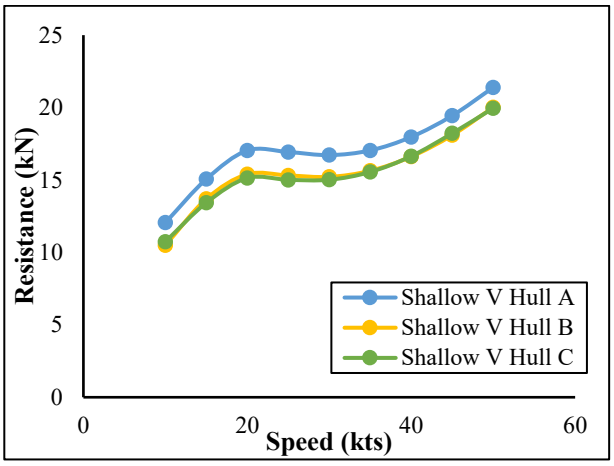

Fig. 12. Resistance vs. speed on the shallow V hull variations.

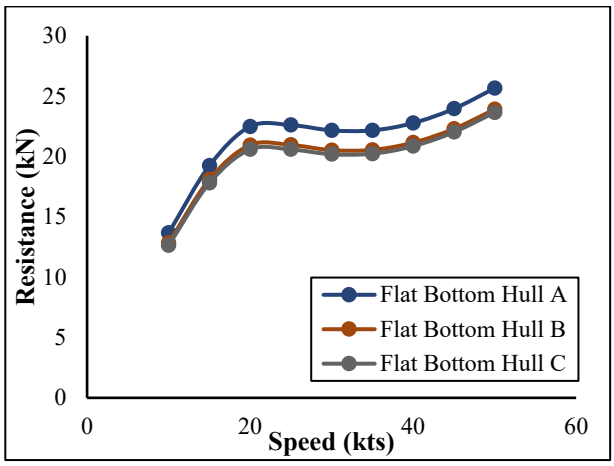

Fig. 13. Resistance vs. speed on the flat bottom hull variations.

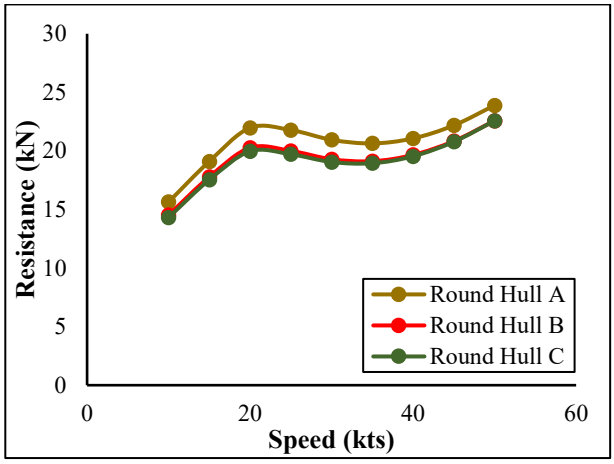

Fig. 14. Resistance vs. speed on the round hull variations.

Table 8. Power result of twelve ship variation.

Speed (kts)	Power (kW)											
	Hull Type											
	Deep V Hull			Shallow V Hull			Flat Bottom Hull			Round Hull		
	A	B	C	A	B	C	A	B	C	A	B	C
10	37.65	33.66	32.95	87.22	71.69	77.69	87.85	82.54	81.21	113.14	105.08	103.59
15	79.78	71.59	70.16	145.29	132.07	129.55	185.48	174.46	171.64	184.31	171.50	169.17
20	133.13	119.66	117.32	219.11	198.01	200.73	289.08	269.40	264.68	282.53	260.69	256.83
25	181.64	163.74	160.78	272.17	246.15	247.37	363.31	336.77	330.84	350.15	321.56	316.91
30	229.15	207.50	204.21	322.49	293.49	295.71	427.50	395.93	389.31	404.07	372.05	367.50
35	284.38	258.73	255.27	392.35	351.88	356.36	498.73	462.37	455.29	464.52	430.33	426.43
40	352.83	322.37	318.79	462.25	427.34	434.83	585.63	543.87	536.38	541.91	505.62	502.70
45	438.01	401.60	397.92	562.62	523.60	534.64	693.13	644.87	636.97	641.87	602.98	601.33
50	542.54	498.82	495.05	687.73	643.49	641.66	824.65	768.52	760.16	768.15	725.85	725.72

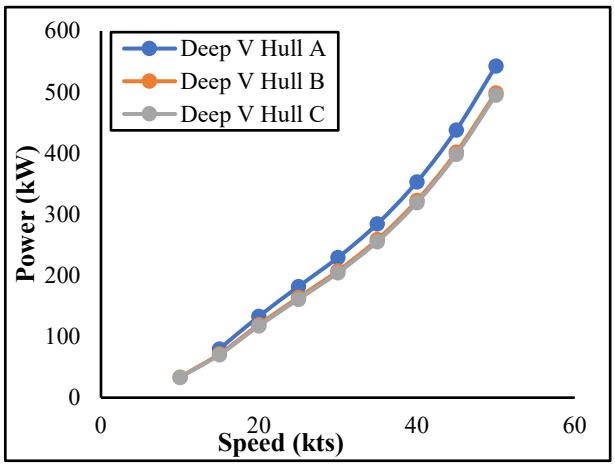

Fig. 15: Power vs. speed on the deep V hull variations.

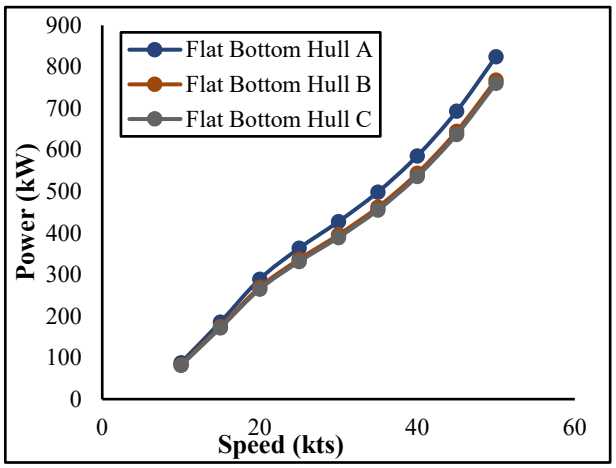

Fig. 17: Power vs. speed on the flat bottom hull variations.

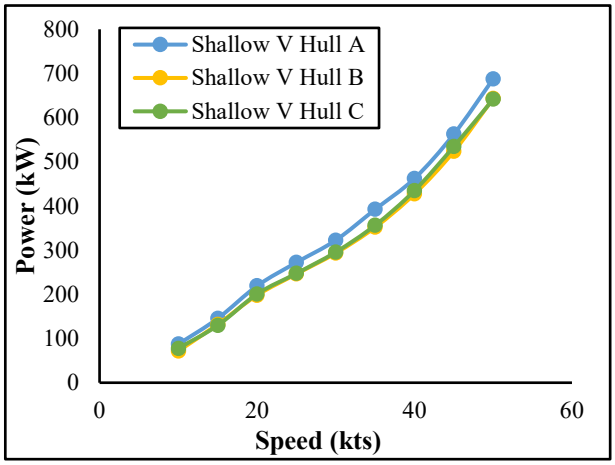

Fig. 16: Power vs. speed on the shallow V hull variations.

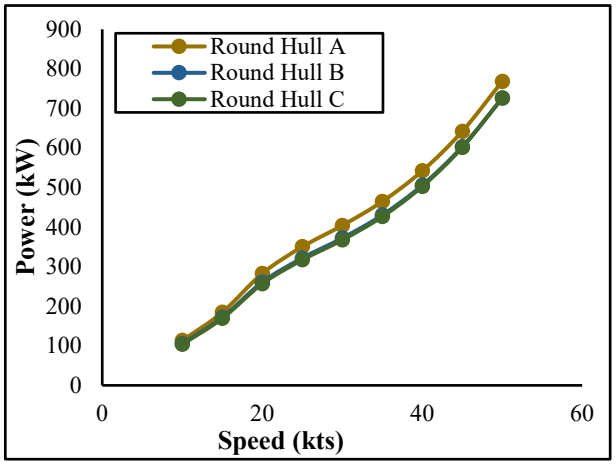

Fig. 18: Power vs. speed on the round hull variations.

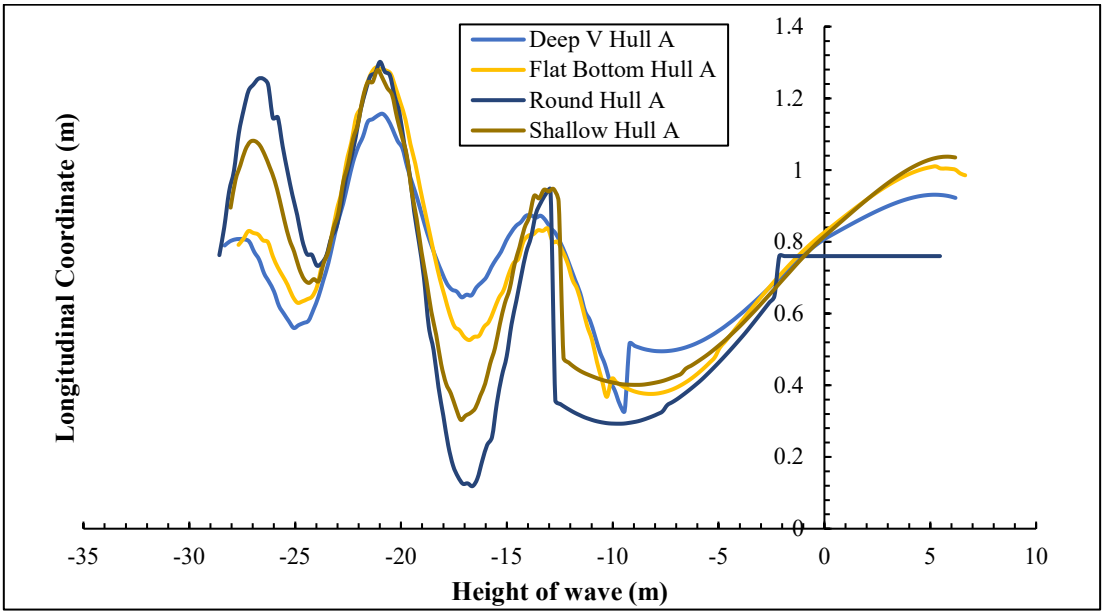

Fig. 19: Wave pattern graphic of Variation 1.

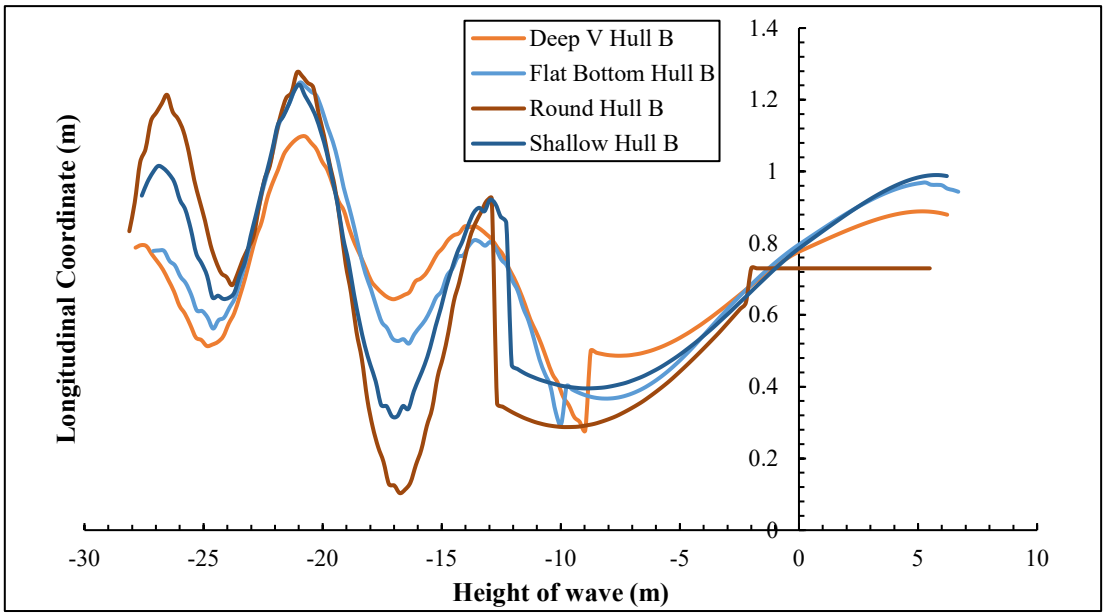

Fig. 20: Wave pattern graphic of Variation 2.

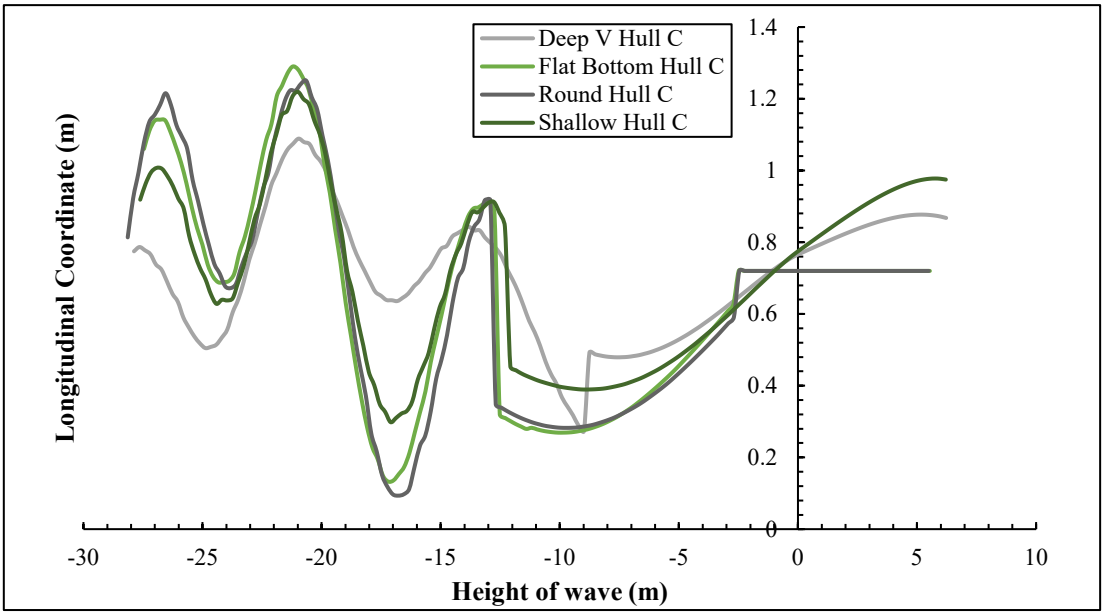

Fig. 21: Wave pattern graphic of Variation 3.

Based on the data above, it was found that each variation with the same hull type with different dimension variations has an almost similar resistance value. Based on Table 7, Hull with the type of Flat Bottom Hull A has the highest resistance value of 22.48 kN at a speed of 20 kts. Meanwhile, the hull with the type of Deep V Hull C has the lowest resistance value of 9.12 kN at a speed of 20 kts.

On the power results, the trend equals the resistance simulation, which is the value of each type of variation in the shape of the same hull with different dimensional variations having a similar value. Based on Table 8, the hull with the type of Flat Bottom Hull A has the highest power value of 289.08 kW at a speed of 20 kts. Meanwhile, the hull with the type of Deep V Hull C has the lowest power value of 117.32 kW at a speed of 20 kts. The increase in resistance value will be directly proportional to the value of power needed.

4.2 Result of Stability Simulation

The ship's stability value was obtained from the comparison of the GZ curve chart with the ship's tilt angle increase. The results of the stability simulation are a graph of the GZ arm and stability value, as shown in Table 9 and Fig. 22.

Table 9. Stability simulation result of twelve ship variations.

Ship	Righting lever curve			
	GZ maximum (m)	α (deg.)	Area (m.deg)	Angle of vanishing point (deg)
Deep V Hull A	0.433	48.2	24.86	94.937
Deep V Hull B	0.44	0.44	25	95.823
Deep V Hull C	0.46	50.9	25.83	95.857
Shallow V Hull A	0.452	39.1	26.08	90.38
Shallow V Hull B	0.452	40.9	26.47	91.139
Shallow V Hull C	0.466	40.9	27.33	91.139
Flat Bottom Hull A	0.347	44.5	18.52	91.266
Flat Bottom Hull B	0.346	46.4	18.4	92.532
Flat Bottom Hull C	0.437	39.1	23.94	88.228

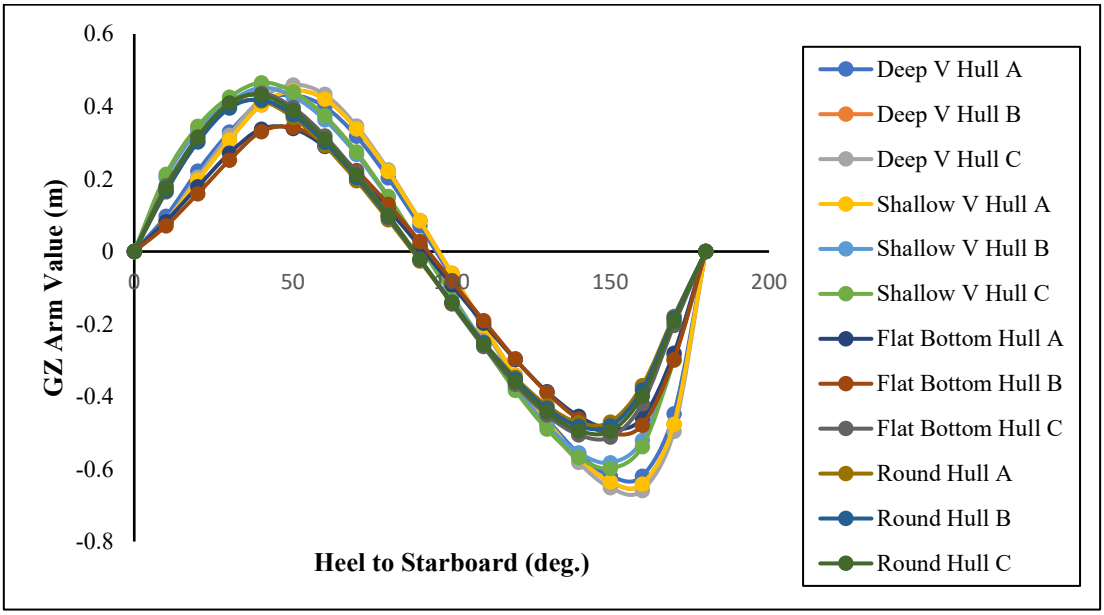

Fig. 22: Righting lever (GZ) graphic of twelve ship variations.

The stability simulation results show that the optimum GZ arm value is obtained by the hull with the type of Shallow V Hull C with a value of 0.466 m, and the largest maximum tilt value is obtained by Deep V Hull C with a value of 50.9 deg. In the largest area, the largest value is obtained by Shallow V Hull C with a value of 27.33 (m.deg), and the largest value of vanishing point is obtained by Shallow V Hull C with a value of 95.857 deg.

4.3 Result of Seakeeping Simulation

Seakeeping analysis was carried out to determine the ship's response to the waves so that the crew and passengers on the ship would be safe and comfortable. In this study, several wave directions were used, including wave direction 90 deg. (beam sea), 135 deg. (bow quartering), 180 deg. (head sea) with a constant speed of 20 kts. The results of the seakeeping simulation will produce RAO graphs on Heaving, Rolling, and Pitching movements. RAO heaving graphic with wave direction 135 deg. at a speed of 20 kts can be seen in Figs. 23-26.

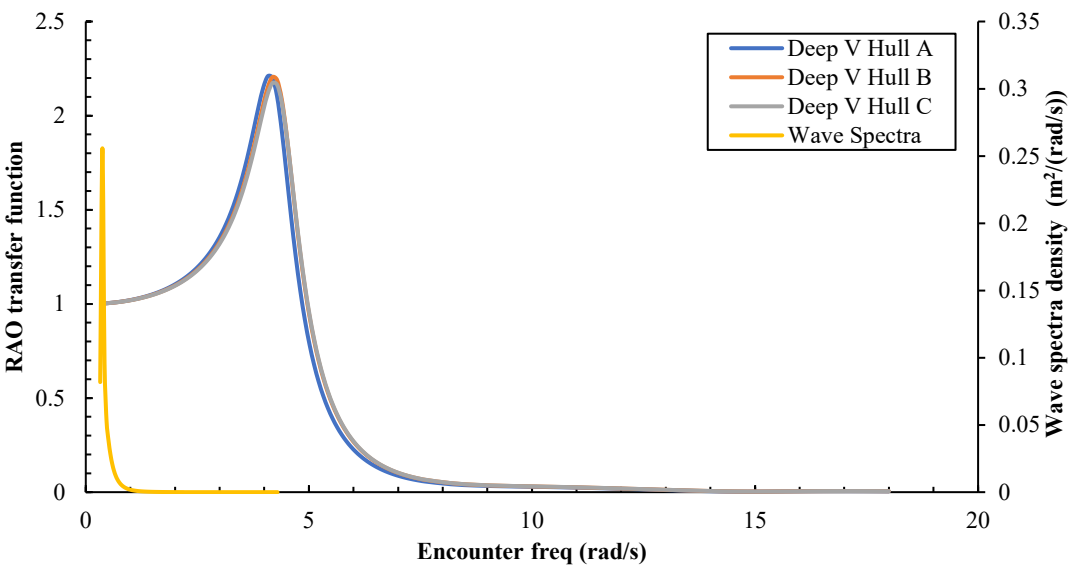

Fig. 23: Heave graphic of deep V hull variations.

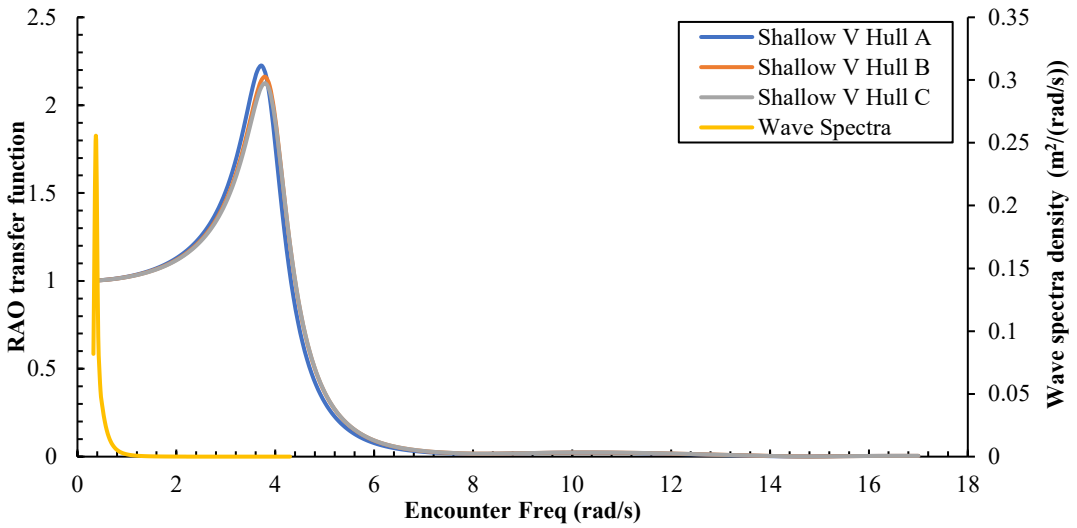

Fig. 24: Heave graphic of shallow V hull variations.

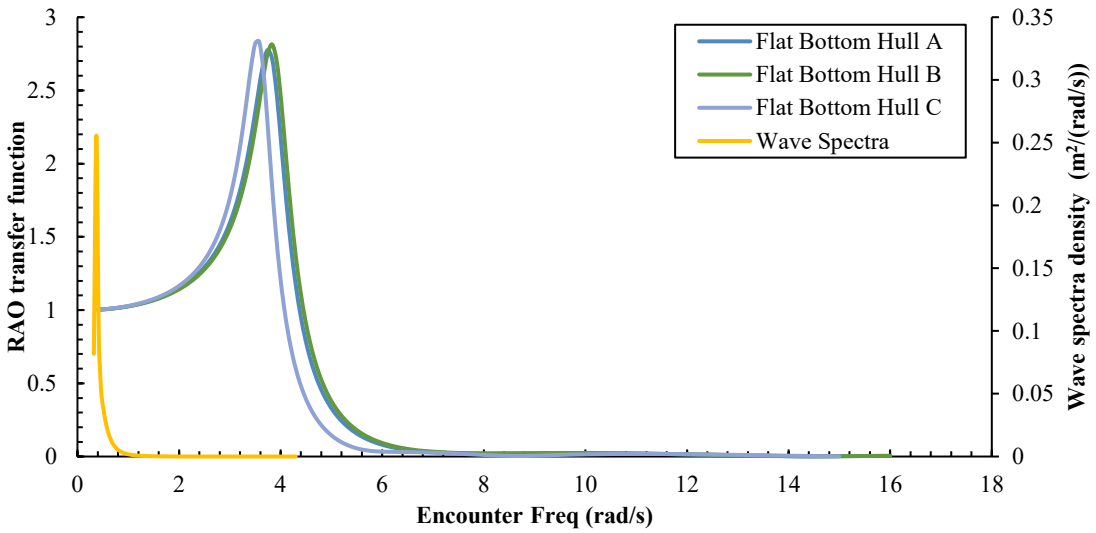

Fig. 25: Heave graphic of flat bottom hull Variations.

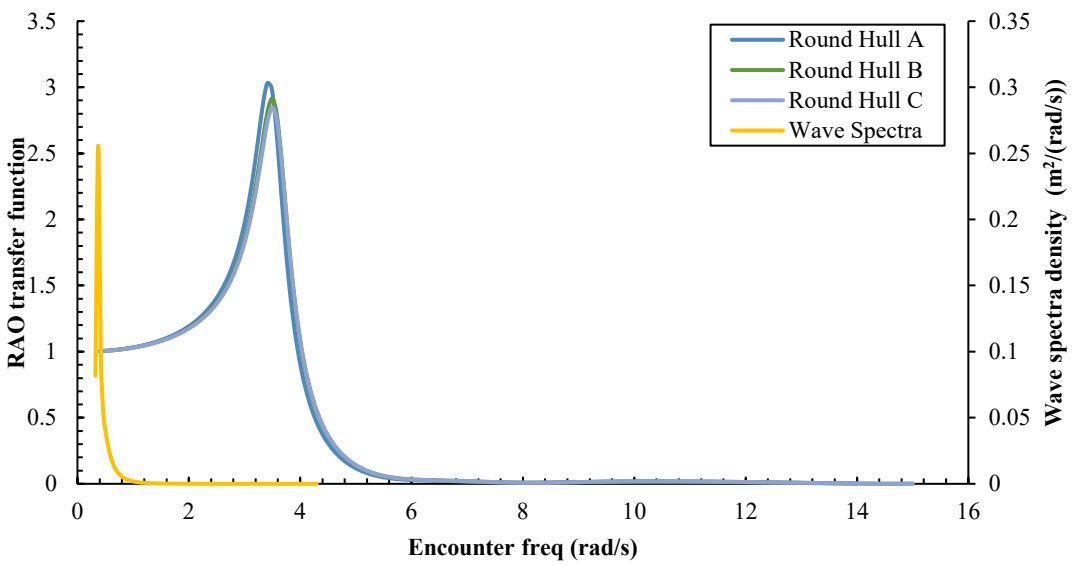

Fig. 26: Heave graphic of round hull variations.

Based on the results above, ships with Deep V, Shallow V, Round Bottom, and Flat Bottom types have similar trend results values when heaving motion. The maximum value of motion response is obtained by ships with the type of Round Hull A at the frequency value of 3.031448 rad/s compared to other types of hulls. Meanwhile, the smallest value is obtained by a ship with the type of Shallow V hull C at a frequency value of 2.125161 rad/s. The round bottom hull has a less good movement response value than other models.

After analyzing seakeeping on heaving motion movement, seakeeping when rolling is analyzed, rolling is a rotating movement to the right or left when the ship is sailing. In this study, rolling movement when waves hit the ship at 135 deg. (bow quartering) at a speed of 20 kts. The RAO charts rolling motion of the twelve hull variations can be seen in Figs. 27-30.

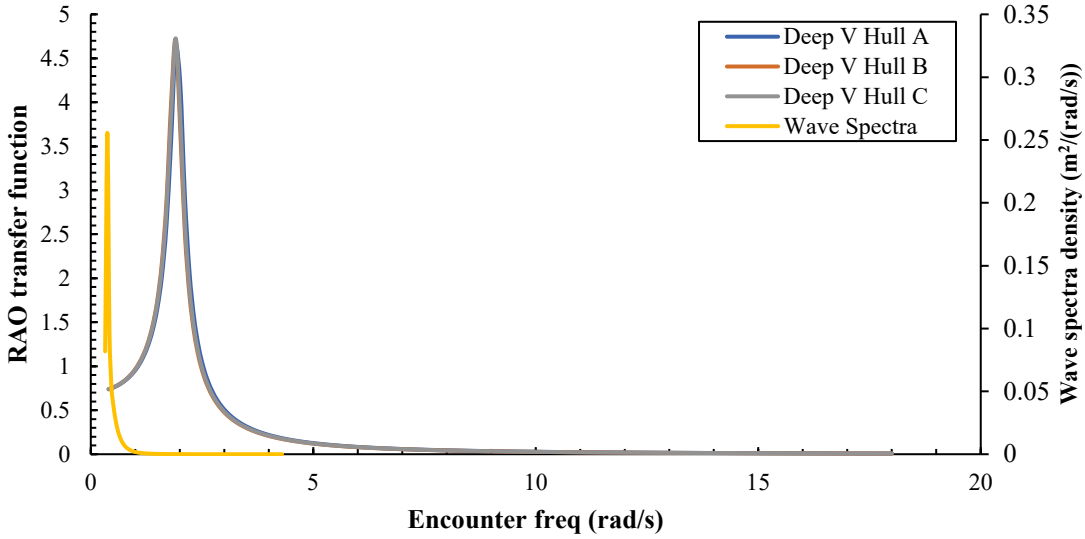

Fig. 27: Roll graphic of deep V hull variations.

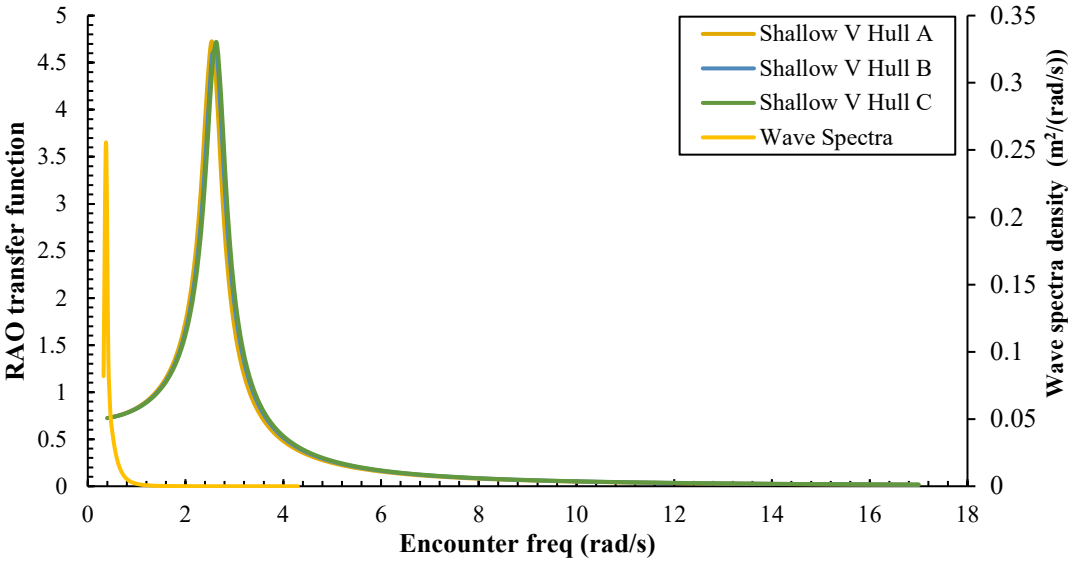

Fig. 28: Roll graphic of shallow V hull variations.

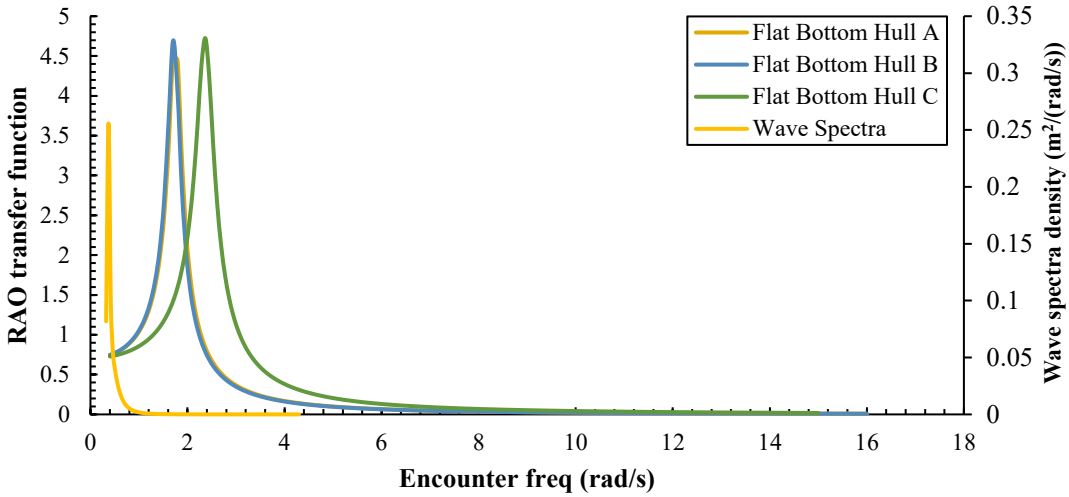

Fig. 29: Roll graphic of flat bottom hull variations.

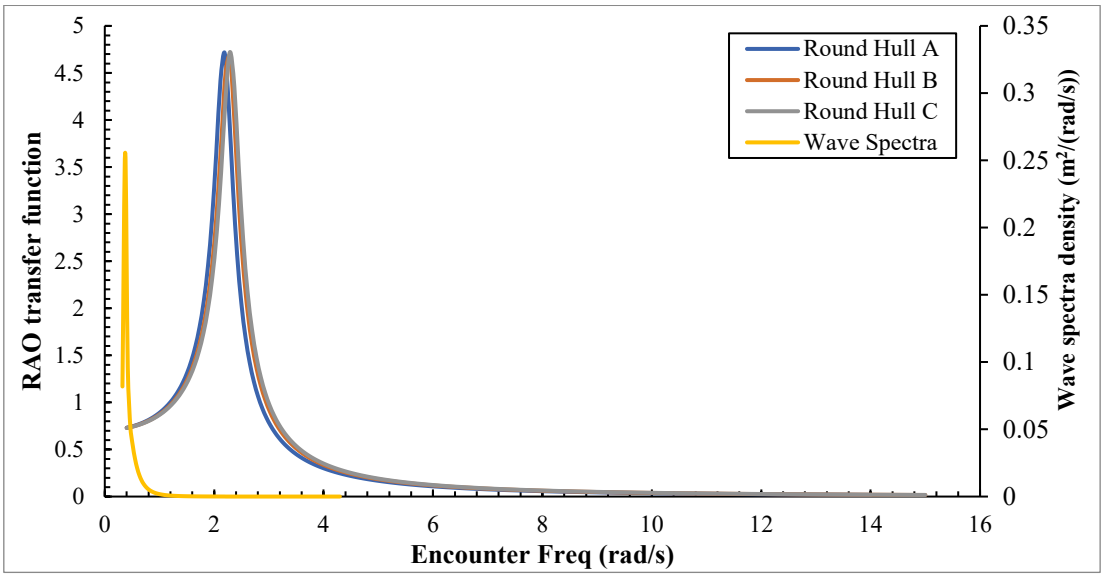

Fig. 30: Roll graphic of round hull variations.

Based on the results of Rolling RAO above, it can be seen that each hull variation has a similar trend. The maximum value of rolling motion response is obtained by ships with the type of Shallow V Hull A at the frequency value of 4.727185 rad/s compared to other types of hulls. Meanwhile, the smallest value is obtained by a ship with the type of Flat Bottom Hull A at a frequency value of 4.473171 rad/s. It can be concluded from the RAO result that the twelve ship rolling variations waves do not experience superposition, which means the ship does not receive no more than one wave simultaneously and makes the ship more stable.

After analyzing seakeeping on heaving and rolling movements, seakeeping on pitching is also analyzed. Pitching is the movement of the ship around the y-axis; when pitching occurs, the bow and stern of the hull will undergo trim changes. In this study, pitching movements when the waves hit the ship at 135 deg. (bow quartering) at a speed of 20 kts. The RAO charts rolling motion of the twelve hull variations can be seen in Figs. 31-34.

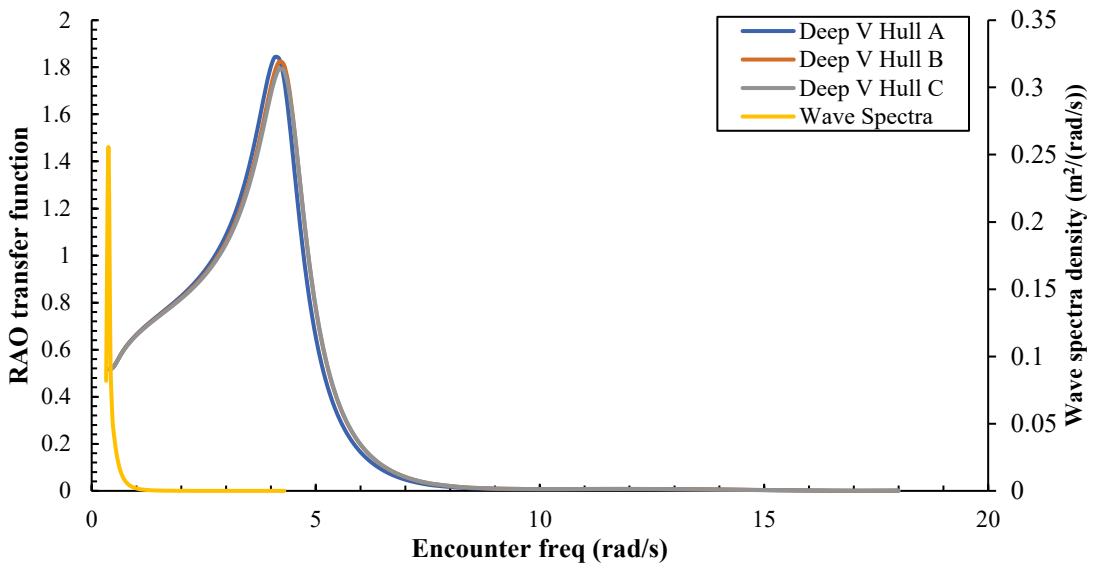

Fig. 31: Pitch graphic of deep V hull variations.

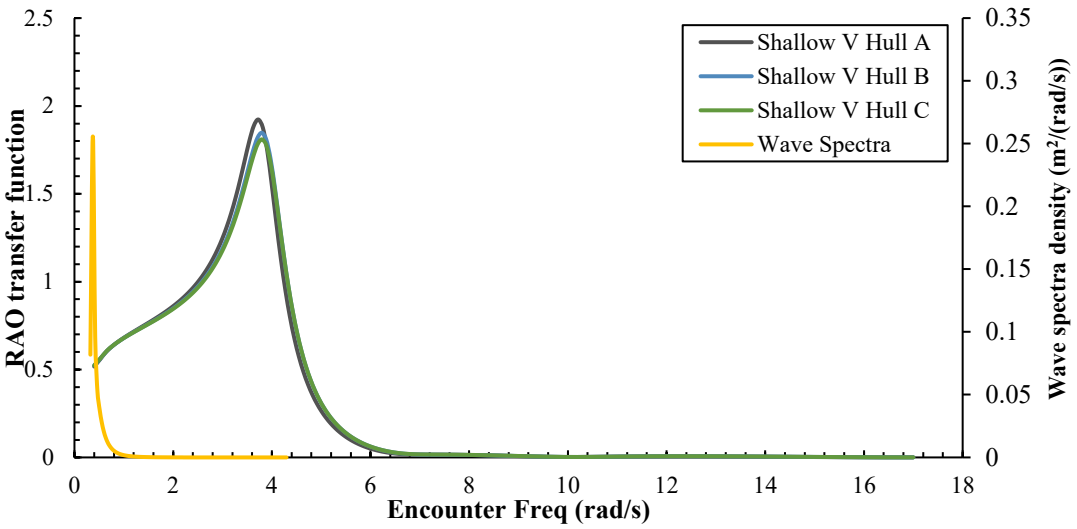

Fig. 32: Pitch graphic of shallow V hull variations.

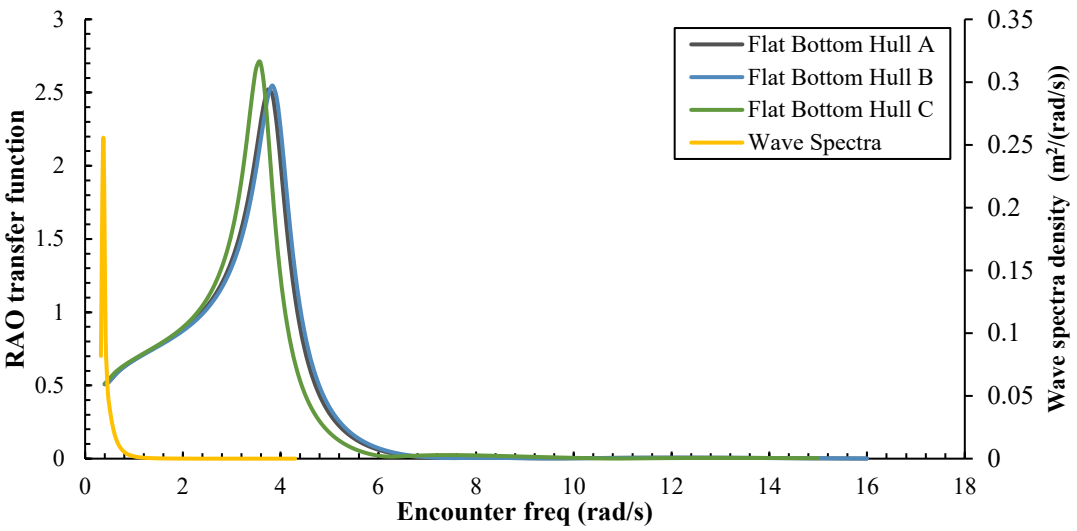

Fig. 33: Pitch graphic of flat bottom hull variations.

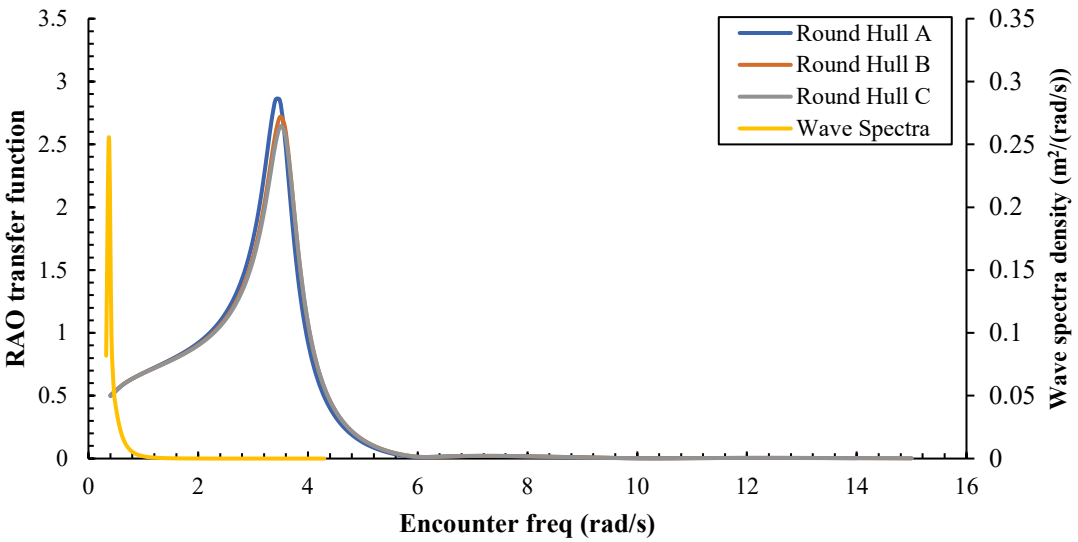

Fig. 34: Pitch graphic of round hull variations.

Based on the results of seakeeping Pitching Motion at a wave direction angle of 135 deg., it can be seen that each hull variation has a similar trend. The minimum pitching response value is obtained by ships with the type Deep V Hull C at the frequency value of 1.792666 rad/s compared to other types of hulls. Meanwhile, the largest pitching value was obtained by ships with the type of Round Hull A at a frequency value of 2.855671 rad/s. It can be concluded from the RAO result on the twelve-ship pitching variation wave superstition does not occur when the ship does not receive more than one wave simultaneously and makes the ship more stable. The following data for seakeeping recapitulation are shown in Table 10.

Table 10. Recapitulation of seakeeping results 135 deg. 20 kts.

Ship	Seakeeping result		
	Heaving (m/m)	Rolling (rad/rad)	Pitching (rad/rad)
Deep V Hull A	2.209854	4.633792	1.842331
Deep V Hull B	2.205313	4.715721	1.824288
Deep V Hull C	2.173162	4.727142	1.792666
Shallow V Hull A	2.224969	4.727185	1.922921
Shallow V Hull B	2.161505	4.631063	1.847311
Shallow V Hull C	2.125161	4.717094	1.809960
Flat Bottom Hull A	2.775198	4.473171	2.520096
Flat Bottom Hull B	2.81374	4.691105	2.548003
Flat Bottom Hull C	2.833001	4.723203	2.711091
Round Hull A	3.031448	4.713931	2.855671
Round Hull B	2.914635	4.678547	2.720904
Round Hull C	2.848650	4.721870	2.643840

4.4 Motion Sickness Incidence (MSI) Result

Leisure boats are ships that used for tourism, where comfort is an important key that must be considered. Motion Sickness Incidence is a comfort parameter of the crew and passengers when the ship sails. The following is the result of a simulation of MS when the ship sails 20 kts with a wave angle of 135 deg. are shown in Table 11 and Figs. 35-38.

Table 11. Motion sickness incidence result.

Ship	MSI ($m.s^{-2}$)
Deep V Hull A	0.179294
Deep V Hull B	0.181735
Deep V Hull C	0.179727
Shallow V Hull A	0.200762
Shallow V Hull B	0.205115
Shallow V Hull C	0.191774
Flat Bottom Hull A	0.195149
Flat Bottom Hull B	0.191507
Flat Bottom Hull C	0.188578
Round Hull A	0.163994
Round Hull B	0.163140
Round Hull C	0.160919

Based on the graph and table above, Round Hull C has the lowest Habitability Acceleration (RMS) value of 0.160919 ms^{-2}, which shows Round Hull C is the safest and does not make passengers experience seasickness. Then, the largest Habitability Acceleration (RMS) value is owned by Shallow V Hull B, which is 0.205115 ms^{-2}. This value is considered to be within the limits of the Not Uncomfortable according to the International Standard

(ISO 2631). The variation of the twelve ships above has a good level of comfort. However, please note that this study used a leisure boat model with an LOA of 9-10 m. Ships with this dimension only operate at a certain time and not for a long time.

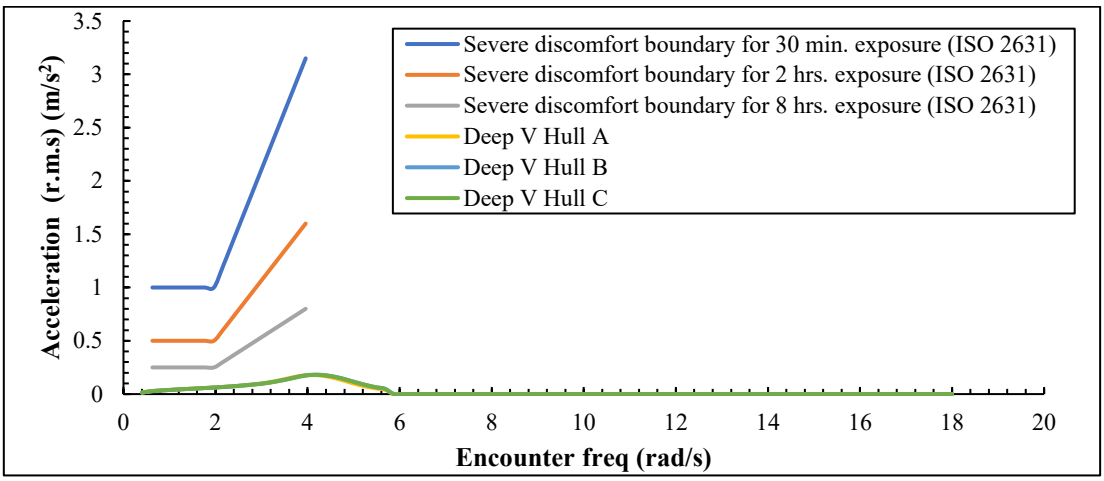

Fig. 35: MSI graphic on deep V hull variations.

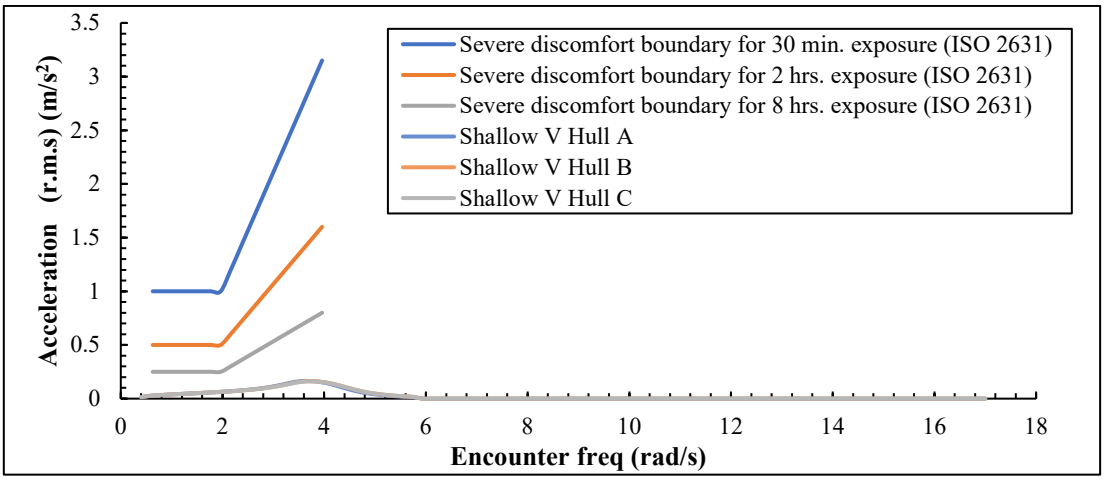

Fig. 36: MSI graphic on shallow V hull variations.

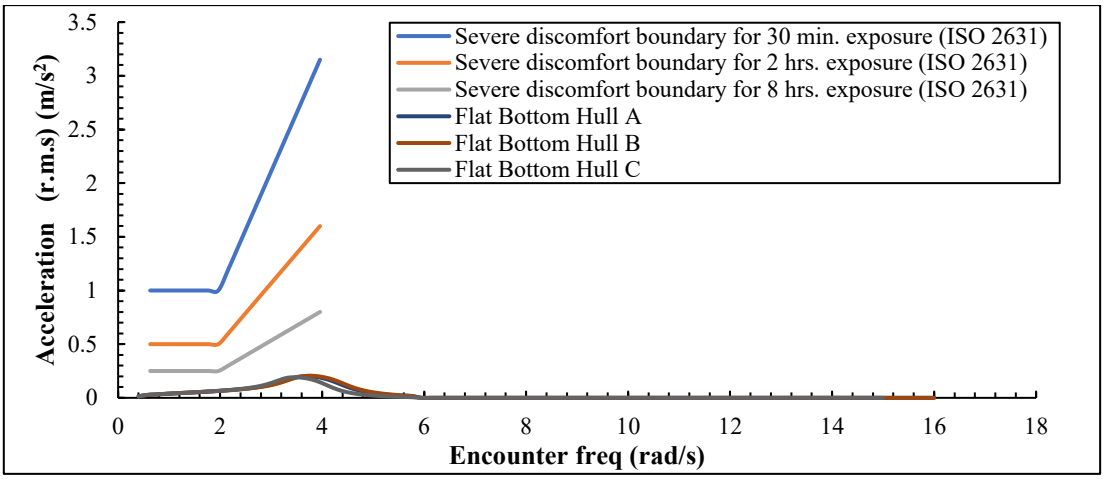

Fig. 37: MSI graphic on flat bottom hull variations.

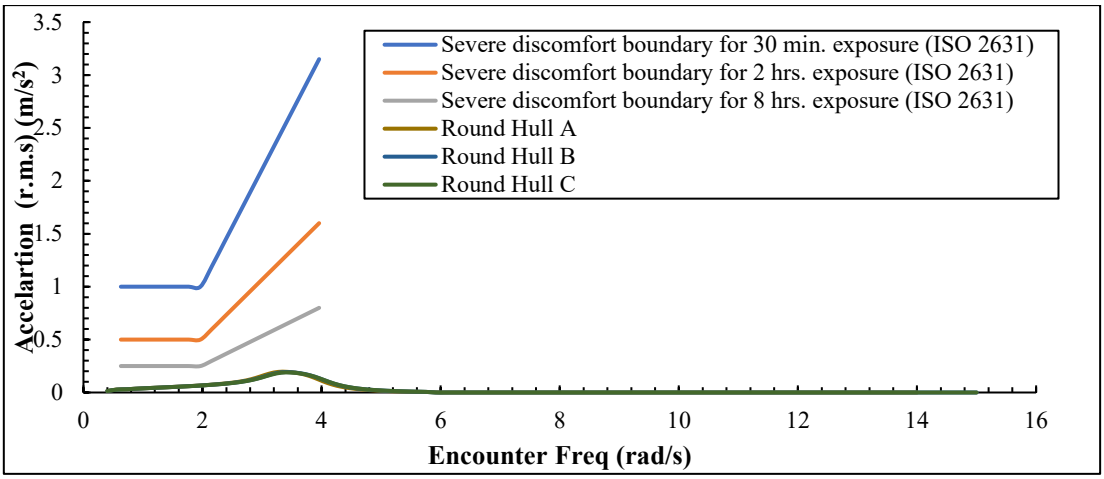

Fig. 38: MSI graphic on round hull variations.

4.5 Slamming & Deck Wetness Result

In the seakeeping analysis, the value of slamming and deck wetness must be minimized because slamming can damage the strength structure of the ship, and deck wetness can reduce the comfort of passengers who are sailing due to splashes of water entering the ship's deck. In this study, the analysis of slamming and deck wetness was carried out when the ship sailed at a speed of 20 kts with a wave angle of 135 deg. The results of slamming and deck wetness simulations can be seen in Table 12.

Table 12. Slamming and deck wetness result of twelve ship variations.

Ship	Criteria	
	Slamming (MII/H)	Deck Wetness (MII/H)
Deep V Hull A	0.149	0.003
Deep V Hull B	0.181	0.005
Deep V Hull C	0.095	0.001
Shallow V Hull A	0.041	0.001
Shallow V Hull B	0.045	0.001
Shallow V Hull C	0.042	0.001
Flat Bottom Hull A	0.065	0.002
Flat Bottom Hull B	0.069	0.003
Flat Bottom Hull C	0.033	0.001
Round Hull A	0.019	0.001
Round Hull B	0.025	0.001
Round Hull C	0.024	0.001

Based on the results of slamming and deck wetness above, hulls with the type of Round Bottom Hull A have the smallest probability value of slamming with a value of 0.019 MII/H, and the probability value of experiencing the smallest deck wetness is obtained by hulls with types of Deep V Hull C, Shallow V Hull A, Shallow V Hull B, Shallow V Hull C. Flat Bottom Hull C, Round Hull A, Round Hull B, and Round Hull C with a value of 0.001 MII/H. This indicates that the probability of the ship experiencing slamming and deck wetness is less than once per hour. Hull with the type Deep V Hull A has the greatest probability value of experiencing slamming with a value of 0.181 MII/H, and the probability value of experiencing the largest deck wetness is obtained by hull with the type of Deep V Hull B with a value of 0.005 MII/H. This shows that the probability of slamming and deck wetness is still less than once per hour.

4.6 Sensitivity Analysis

In sensitivity analysis, this study uses a linear regression method approach to obtain coefficient, standard error, and significant F values to determine the influence of variations in hull dimensions and shape. In this study, the block coefficient and simulation results were used as input data from hull-type variation. In contrast, the displacement volume value and simulation results were used as input data from dimension variation. The greater the value of R indicates that a variable influences hydrodynamic criterion. The indicator coefficient indicates the number of changes x that must be multiplied to produce the average change of y for each increment of unit x. In this way, it can represent the slope of the line up or down. The higher the value of the coefficient means, the less influence the variation has on the yield.

The regression standard error shows the average distance of observed values from the regression line. However, this can show that there is an error in the regression model on average using response variables, so the higher the standard error value. Thus, the smaller the effect of changing variations on the final result. The P-value indicator shows the probability of observation of the value of the coefficient. The smaller the p-value, the

smaller the effect of variation on the final result. The significant F in regression is a test of linear regression models in providing a better fit to the data set than models without predictor variables. The smaller the significant value of F, the greater the influence of variation on the final result. The results of sensitivity analysis on the resistance value criteria can be seen in Table 13.

Table 13. Sensitivity analysis on the resistance result.

Resistance		
Indicator	Variable	
	Hull Type	Hull Size
Coefficient	584.7884	16.61331
Standard Error	29.05472	38.27914
P - Values	6.18E-05	0.001048
R Square	0.812711	0.674909
Significant F	6.18E-05	0.001048

Based on the table above, the value of the hull shape has a significant influence because it has the largest R-value and the smallest significant F-value. In addition, the greater the coefficient, standard error, and p-values indicate that dimensional variations have little effect on the final result. The results of sensitivity analysis on stability criteria can be seen in Table 14.

Table 14. Sensitivity analysis on the stability results.

Stability		
Indicator	Variable	
	Hull Type	Hull Size
Coefficient	-13.625195	-0.1993
Standard Error	2.67610969	2.951667
P - Values	0.12660996	0.49459
R Square	0.21732805	0.047847
Significant F	0.12660996	0.49459

Based on the table above, the value of the hull shape has a significant influence because it has the largest R-value and the smallest significant F-value. In addition, the greater the coefficient, standard error, and p-values indicate that dimensional variations have little effect on the final result. The results of sensitivity analysis on Heave motion criteria can be seen in Table 15.

Table 15. Sensitivity analysis on the heaving motion.

Heave Motion		
Indicator	Variable	
	Hull Type	Hull Size
Coefficient	3.34661398	0.087361
Standard Error	0.16170938	0.249002
P - Values	4.8992E-05	0.004223
R Square	0.82103691	0.575676
Significant F	4.8992E-05	0.004223

Based on the table above, the value of the hull shape has a significant influence because it has the largest R-value and the smallest significant F-value. In addition, the greater the coefficient, standard error, and p-values indicate that dimensional variations have little effect on the final result. The results of sensitivity analysis on the Roll Motion criteria can be seen in Table 16.

Table 16. Sensitivity on the roll motion result.

Roll Motion		
Indicator	Variable	
	Hull Type	Hull Size
Coefficient	0.02607747	0.002832
Standard Error	0.07696058	0.076432
P - Values	0.91389094	0.705388
R Square	0.00122834	0.014911
Significant F	0.91389094	0.705388

Based on the table above, the value of the hull size has a significant influence because it has the largest R-value and the smallest significant F-value. In addition, the greater the coefficient, standard error, and p-values indicating variations in hull shape have little effect on the final result. The results of sensitivity analysis on the Pitch Motion criteria can be seen in Table 17.

Table 17. Sensitivity analysis on the pitch motion result.

Pitch Motion		
Indicator	Variable	
	Hull Type	Hull Size
Coefficient	4.16565135	0.111519
Standard Error	0.16688997	0.276866
P - Values	9.7976E-06	0.001747
R Square	0.86968401	0.641345
Significant F	9.7976E-06	0.001747

Based on the table above, the value of the hull shape

has a significant influence because it has the largest R-value and the smallest significant F-value. In addition, the greater the coefficient, standard error, and p-values indicate that dimensional variations have little effect on the final result. The results of sensitivity analysis on the criteria of Motion Sickness Incidence (MSI) can be seen in Table 18.

Table 18. Sensitivity analysis on the MSI result.

Motion Sickness Incidence (MSI)		
Indicator	Variable	
	Hull Type	Hull Size
Coefficient	0.07885485	0.001264977
Standard Error	0.013164828	0.014909133
P - Values	0.0783855	0.3939884
R Square	0.277619908	0.073511238
Significant F	0.078385517	0.393988424

Based on the table above, the value of the hull shape has a significant influence because it has the largest R-value and the smallest significant F-value. In addition, the greater the coefficient, standard error, and p-values indicate that dimensional variations have little effect on the final result. The results of sensitivity analysis on the slamming criteria can be seen in Table 19.

Table 19. Sensitivity analysis on the slamming result.

Slamming		
Indicator	Variable	
	Hull Type	Hull Size
Coefficient	-0.418262274	-0.013943095
Standard Error	0.032571862	0.028144546
P - Values	0.001820686	0.000400684
R Square	0.638509574	0.730101709
Significant F	0.001820686	0.000400684

Based on the table above, the value of the hull size has a significant influence because it has the largest R-value and the smallest significant F-value. In addition, the greater the coefficient, standard error, and p-values indicating variations in hull shape have little effect on the final result. The results of sensitivity analysis on the Deck Wetness criteria can be seen in Table 20.

Table 20. Sensitivity analysis on the deck wetness result.

Deck Wetness		
Indicator	Variable	
	Hull Type	Hull Size
Coefficient	-0.009134871	-0.000355778
Standard Error	0.001315733	0.001108998
P - Values	0.046389638	0.007145144
R Square	0.340513199	0.531475212
Significant F	0.046389638	0.007145144

Based on the table above, the value of the hull size has a significant influence because it has the largest R-value and the smallest significant F-value. In addition, the greater the coefficient, standard error, and p-values indicating variations in hull shape have little effect on the final result.

4.7 Multi-Attribute Decision Making (MADM)

The best design is selected using MADM method based on its hydrodynamic characteristics. In the MADM analysis, two leisure boats that operating around the Lombok Island were analyzed to validate the simulation results. The two leisure boats that analyzed are the Yacht Accura 55 and the Yacht Kelana. The main dimensions of the boats are shown in Table 21.

Table 21. Ship reference for model validation.

Model Validation	Parameter	Value
Yacht Kelana	LOA (m)	15.50
	Beam (m)	4.75
	Depth (m)	3.50
	Draft (m)	1.75
Yacht Accura 55	LOA (m)	17.00
	Beam (m)	3.90
	Depth (m)	3.20
	Draft (m)	1.30

The first stage in this MADM method is to determine the sequence and give a score based on its importance on each parameter of hydrodynamic characteristics. The weighting, score, and importance in each parameter of this criterion must adjust to the vessel's operational needs. The multi-attribute decision making score and importance can be seen in Table 22.

Table 22. Multi-Attribute decision making scoring and importance.

Parameter	Value
Very important	5 Points
Quite important	4 Points
Important	3 Points
Not important	2 Points
Very unimportant	1 Points

In this study, resistance valued 2 points (Not Important) because leisure ships are intended for travel, so speed is not important factor. Deck wetness and slamming valued 3 points (Important), to make sure that the ships are reliable for sailing through many water conditions. MSI valued 4 points (Quite Important) because it is considered important for passenger safety when the ship sails. Therefore, stability, heaving, rolling, and pitching valued 5 points (Very Important) because they play an important role in the safety and comfort of passengers when the ship sails. The MADM total score in percent on each parameter are shown in Table 23.

Table 23. Multi-attribute decision making parameter.

Criteria	Parameter	Value	Score (%)
Resistance (C1)	Not Important	2 Points	6.250
Stability (C2)	Very Important	5 Points	15.625
Heaving (C3)	Very Important	5 Points	15.625
Rolling (C4)	Very Important	5 Points	15.625
Pitching (C5)	Very Important	5 Points	15.625
MSI (C6)	Quite Important	4 Points	12.500
Slamming (C7)	Important	3 Points	9.375
Deck Wetness (C8)	Important	3 Points	9.375

The resistance value in this data is taken when the ship operates at a speed of 20 kts. The stability value is based on the Area Under GZ Curve. In the seakeeping parameter, the value taken is the highest value on the RAO chart in each movement, including heaving, rolling, and pitching. Meanwhile, the Motion Sickness Incidence (MSI) parameter was taken as the highest value on the MSI chart at a speed of 20 kts and a wave angle of 135 deg. The slamming and deck wetness values are taken when the ship is operating at a speed of 20 kts and a wave angle of 135 deg. Data from twelve ship variation models for MADM analysis can be seen in Table 24.

Table 24. Multi-Attribute decision making parameters value.

Model	Criteria							
	Resistance	Stability	Seakeeping			MSI	Slamming	Deck wetness
	C1	C2	C3	C4	C5	C6	C7	C8
Deep V Hull A	10.350	24.860	2.210	4.630	1.840	0.179	0.149	0.004
Deep V Hull B	9.300	25.000	2.210	4.720	1.820	0.181	0.181	0.005
Deep V Hull C	9.120	25.830	2.170	4.730	1.790	0.179	0.095	0.002
Shallow V Hull A	17.040	26.080	2.220	4.730	1.920	0.163	0.041	0.001
Shallow V Hull B	15.400	26.470	2.160	4.630	1.850	0.163	0.045	0.002
Shallow V Hull C	15.130	27.330	2.130	4.720	1.810	0.160	0.042	0.002
Flat Bottom Hull A	22.480	18.520	2.780	4.470	2.520	0.200	0.065	0.002
Flat Bottom Hull B	20.950	18.400	2.810	4.690	2.550	0.205	0.069	0.005
Flat Bottom Hull C	20.580	23.940	2.830	4.720	2.710	0.191	0.033	0.001
Round Hull A	21.970	22.440	3.030	4.710	2.860	0.195	0.019	0.001
Round Hull B	20.270	22.760	2.910	4.680	2.720	0.191	0.025	0.001
Round Hull C	19.970	23.570	2.850	4.720	2.640	0.188	0.024	0.001
Yacht Accura 55	66.110	11.030	2.190	4.720	1.890	0.391	0.348	0.003
Yacht Kelana	109.910	17.120	2.540	4.720	2.350	0.429	0.807	0.018

Then, the next stage is normalizing the data to avoid data anomalies. In the criteria C1 (resistance), C3-C5 (seakeeping), C6 (MSI), C8 (slamming), and C8 (deck wetness) the smallest data is taken. Because the smaller the resistance value and the smaller the peak point value of RAO, MSI, slamming, and deck wetness, the ship is considered better. In contrast, the C2 criterion takes the largest value as a parameter because a good ship has a large area value Under the GZ Area. The results of data normalization on twelve variation vessels are shown in Table 25.

Table 25. Multi-Attribute decision making data normalization.

Model	**Criteria**							
	C1 (Min)	**C2 (Max)**	**C3 (Min)**	**C4 (Min)**	**C5 (Min)**	**C6 (Min)**	**C7 (Min)**	**C8 (Min)**
Deep V Hull A	0.881	0.910	0.962	0.965	0.973	0.898	0.128	0.250
Deep V Hull B	0.980	0.915	0.964	0.949	0.983	0.885	0.105	0.200
Deep V Hull C	1.000	0.945	0.978	0.946	1.000	0.895	0.200	0.500
Shallow V Hull A	0.535	0.954	0.955	0.946	0.932	0.981	0.463	1.000
Shallow V Hull B	0.593	0.969	0.983	0.966	0.970	0.986	0.422	0.500
Shallow V Hull C	0.603	1.000	1.000	0.948	0.990	1.000	0.452	0.500
Flat Bottom Hull A	0.406	0.678	0.766	1.000	0.711	0.802	0.292	0.500
Flat Bottom Hull B	0.435	0.673	0.755	0.954	0.704	0.785	0.275	0.200
Flat Bottom Hull C	0.443	0.876	0.750	0.947	0.661	0.839	0.576	1.000
Round Hull A	0.415	0.821	0.701	0.949	0.628	0.825	1.000	1.000
Round Hull B	0.450	0.833	0.729	0.956	0.659	0.840	0.760	1.000
Round Hull C	0.457	0.862	0.746	0.947	0.678	0.853	0.792	1.000
Yacht Accura 55	0.138	0.404	0.972	0.947	0.949	0.411	0.055	0.333
Yacht Kelana	0.083	0.626	0.838	0.947	0.762	0.375	0.024	0.056

Table 26. Multi-Attribute decision making total result.

Model	Criteria								
	C1	C2	C3	C4	C5	C6	C7	C8	Total Weight
Deep V Hull A	0.055	0.142	0.1503	0.1508	0.1520	0.1122	0.0120	0.0234	0.798
Deep V Hull B	0.061	0.143	0.1506	0.1482	0.1535	0.1107	0.0098	0.0188	0.796
Deep V Hull C	0.063	0.148	0.1528	0.1479	0.1563	0.1119	0.0188	0.0469	0.845
Shallow V Hull A	0.033	0.149	0.1492	0.1479	0.1457	0.1227	0.0434	0.0938	0.885
Shallow V Hull B	0.037	0.151	0.1536	0.1509	0.1516	0.1233	0.0396	0.0469	0.854
Shallow V Hull C	0.038	0.156	0.1563	0.1482	0.1548	0.1250	0.0424	0.0469	0.867
Flat Bottom Hull A	0.025	0.106	0.1197	0.1563	0.1111	0.1002	0.0274	0.0469	0.693
Flat Bottom Hull B	0.027	0.105	0.1180	0.1490	0.1099	0.0981	0.0258	0.0188	0.652
Flat Bottom Hull C	0.028	0.137	0.1172	0.1480	0.1033	0.1049	0.0540	0.0938	0.786
Round Hull A	0.026	0.128	0.1095	0.1483	0.0981	0.1031	0.0938	0.0938	0.801
Round Hull B	0.028	0.130	0.1139	0.1494	0.1029	0.1050	0.0713	0.0938	0.795
Round Hull C	0.029	0.135	0.1166	0.1480	0.1059	0.1067	0.0742	0.0938	0.808
Yacht Accura 55	0.009	0.063	0.1520	0.1479	0.1483	0.0514	0.0051	0.0313	0.608
Yacht Kelana	0.005	0.098	0.1309	0.1480	0.1191	0.0468	0.0022	0.0052	0.555

Upon completing the data normalization stage, the calculation of the MADM assessment can be carried out. The model that has the highest score value is considered the best model. The MADM total scores are presented in Table 26.

After obtaining the total score from twelve variation models, ranking is conducted to determine the best model that has the largest final score. The ranking results for the twelve ship variation models can be seen in Table 27.

Based on these results, it can be concluded that the Shallow V Hull A model exhibits the best hydrodynamic performances, with a final score of 0.885. In comparison, the model with the smallest hydrodynamic performances is the Yacht Kelana, with a final score of 0.555.

Table 27. Multi-Attribute decision making ranking result.

Model	Total Score	Ranking
Shallow V Hull A	0.885	1
Shallow V Hull C	0.867	2
Shallow V Hull B	0.854	3
Deep V Hull C	0.845	4
Round Hull C	0.808	5
Round Hull A	0.801	6
Deep V Hull A	0.798	7
Deep V Hull B	0.796	8
Round Hull B	0.795	9
Flat Bottom Hull C	0.786	10
Flat Bottom Hull A	0.693	11
Flat Bottom Hull B	0.652	12
Yacht Accura 55	0.608	13
Yacht Kelana	0.555	14

5. Conclusions

The sensitivity analysis results indicate that variations in hull shape significantly impact resistance, stability, heave motion, roll motion, and motion sickness incidence (MSI) values more than dimension variations. However, changes in hull dimensions have a more substantial effect on pitch motion, slamming, and deck wetness than hull shape.

In the multi-attribute decision making (MADM) analysis result in this research, it was found that variation of hull dimension and hull shape has a similar trend. Hull variations that have the best hydrodynamic performances consecutively are Shallow V Hull A, Shallow V Hull C, Shallow V Hull B, Deep V Hull C, Round Hull C, Round Hull A, Deep V Hull A, Deep V Hull B, Round Hull B, Flat Bottom Hull C, Flat Bottom Hull A, Flat Bottom Hull B, Yacht Accura 55, Yacht Kelana.

Further research is needed on the hydrodynamic characteristics of ship hulls, considering the superstructure and propulsion components. This study focused solely on the hull, without including the superstructure and propulsion components.

The result of this research has significant implications for the maritime industry, particularly in terms of design, efficiency, safety, and the tourism experience. This research assists leisure boat manufacturers in designing vessels that are efficient, stable, and comfortable, tailored to the operational needs of the boats.

Nomenclature

C_f	Coefficient of frictional resistance
C_v	Coefficient of viscous resistance
F_n	Froude number
G	Center of gravity
g	Gravity acceleration (m/s^2)
GZ	Distance of point G to Z (m)
K	Turbulence kinetic energy (m^2/s^2)
L	Length of waterline (m)
m_4	Spectral moment of the ship
R_f	Frictional resistance (N)
R_n	Reynold number
R_v	Viscous resistance (N)
R_w	Wave resistance (N)
S	Wetted area (m^2)
V	Displacement volume (m^3)
v	Speed (m/s)

Greek symbols

Δ	Displacement (kg)
β	Deadrise angel (deg)
ζ_a	Amplitude of the incident wave (deg)
$\emptyset_a$	Ship motion response amplitude
λ	Leeway angle (deg)
μ	Water viscosity (m^2/s)
ρ	Water density(kg/m^3)
τ	Trim angel (deg)
φ	Heel angle (deg)

References

1) I. Ismayanti, "Mapping seascapes tourism destination in Indonesia," *Jurnal Industri Pariwisata*, **1** (*1*) 71–80 (2018). doi:10.36441/pariwisata.v1i1.17.
2) Kementrian Pariwisata Republik Indonesia, "Rencana strategis kementrian pariwisata tahun 2015 - 2019," (2015). www.jdih.kemenparekraf.go.id (accessed October 10, 2023).
3) M.T. Astuti, "Strategi pengembangan wisata bahari di gili trawangan kabupaten lombok barat provinsi nusa tenggara barat," National Conference of Creative Industry Universitas Bunda Mulia, Jakarta, 2018.
4) A. Pratama, A. Prabowo, T. Tuswan, R. Adiputra, N. Muhayat, B. Cao, S. Hadi, and I. Yaningsih, "Fast patrol boat hull design concepts on hydrodynamic performances and survivability evaluation," *J. Appl. Eng. Sci.*, **21** (*2*) 501–531 (2023). doi:10.5937/jaes0-40698.
5) H. Nubli, F.S. Utomo, H. Diatmaja, A.R. Prabowo, U. Ubaidillah, D.D. Susilo, W. Wibowo, T. Muttaqie, and F.B. Laksono, "Design of the bengawan unmanned vehicle (uv) roboboat: mandakini neo," *Mekanika: Majalah Ilmu Mekanika*, **21** (*2*) 64-74 (2022). doi:10.20961/mekanika.v21i2.61624.
6) D.R. Mandasari, K. Yulianto, L. Amelia, A. Aziz, E.D. Purnomo, Faisal, and C.S.A. Nandar, "Design and optimization of brushless dc motor for electric boat thruster," *Evergreen*, **10** (*3*) 1928–1937 (2023). doi:10.5109/7151773.
7) W. Zayat, H.S. Kilic, A.S. Yalcin, S. Zaim, and D. Delen, "Application of madm methods in industry 4.0: a literature review," *Comput. Ind. Eng.*, **177** 109075 (2023). doi:10.1016/j.cie.2023.109075.
8) T. Rahmaji, A.R. Prabowo, T. Tuswan, T. Muttaqie, N. Muhayat, and S.J. Baek, "Design of fast patrol boat for improving resistance, stability, and seakeeping performance," *Designs*, **6** (*6*) 105 (2022). doi:10.3390/designs6060105.
9) Y.S. Yang, C.K. Park, K.H. Lee, and J.C. Suh, "A study on the preliminary ship design method using deterministic approach and probabilistic approach including hull form," *Struct. Multidiscip. Optim.*, **33** (*6*) 529–539 (2007). doi:10.1007/s00158-006-0063-5.
10) R. Campbell, M. Terziev, T. Tezdogan, and A. Incecik, "Computational fluid dynamics predictions of draught and trim variations on ship resistance in confined waters," *Appl. Ocean Res.*, **126** 103301 (2022). doi:10.1016/j.apor.2022.103301.

11) D.A.H. Molland, Anthony F., Stephen R. Turnock, "Ship Resistance and Propulsion," 2nd Ed, Cambridge University Press, Cambridge, 2017.
12) D.M. Prabowoputra, A.R. Prabowo, I. Yaningsih, D.D.D.P. Tjahjana, F.B. Laksono, R. Adiputra, and H. Suryanto, "Effect of blade angle and number on the performance of bánki hydro-turbines: assessment using cfd and fda approaches," *Evergreen*, **10** (*1*) 519–530 (2023). doi:10.5109/6782156.
13) M.F. Syahrudin, M.A. Budiyanto, and M.A. Murdianto, "Analysis of the use of stern foil on the high speed patrol boat on full draft condition," *Evergreen*, **7** (*2*) 262–267 (2020). doi:10.5109/4055230.
14) E. Sancak, and F. Çakici, "Determination of the optimum trim angle of a planing hull for minimum drag using savitsky method," *Gemi ve Deniz Teknol.*, (*220*) 43–53 (2021). doi:10.54926/gdt.951371.
15) D.B. Uhls, "Does the Fast Patrol Boat Have a Future in the Navy?," U.S. Army Command and General Staff College, Fort Leavenworth, 2002.
16) A.R. Prabowo, R.A. Febrianto, T. Tuswan, and D.D.D.P. Tjahjana, "Performance evaluation on the designed v-shaped monohull ship models," *J. Appl. Eng. Sci.*, **20** (*2*) 610–624 (2022). doi:10.5937/jaes0-35481.
17) J. Holtrop, and G.G.J. Mennen, "An approximate power prediction method," *Int. Shipbuild. Prog.*, **29** (*335*) 166–170 (1982). doi: -
18) R.I. Julianto, A.R. Prabowo, N. Muhayat, T. Putranto, and R. Adiputra, "Investigation of hull design to quantify resistance criteria using holtrop's regression-based method and savitsky's mathematical model: A study case of fishing vessels," *J. Eng. Sci. Technol.*, **16** (*2*) 1426-1443 (2021). doi: -
19) B. Barrass, and D.R. Derrett, "Ship stability for Masters and Mates," Butterworth-Heinemann, Oxford, 2006.
20) A. Biran, and R. López-Pulido, "Ship hydrostatics and stability," Butterworth-Heinemann, Oxford, 2013.
21) P. Ruponen, "Principles of Ship Buoyancy and Stability," Aalto University, Aalto, 2021.
22) A. Afriantoni, R. Romadhoni, and B. Santoso, "Study on the stability of high speed craft with step hull angle variations," *IOP Conf. Ser. Earth Environ. Sci.*, **430** (*1*) 012040 (2020). doi:10.1088/1755-1315/430/1/012040.
23) N. Nurhasanah, B. Santoso, R. Romadhoni, and P. Nasutioni, "Seakeeping analysis of hull rounded design with multi-chine model on fishing vessel," *IOP Conf. Ser. Earth Environ. Sci.*, **430** (*1*) 012041 (2020). doi:10.1088/1755-1315/430/1/012041.
24) M.L. Ramadiansyah, E. Yazid, M. Mirdanies, Rahmat, B. Azhari, and M.F. Hikmawan, "Motor sizing of a ship-mounted two-dof manipulator system considering variations of ocean wave direction," *Evergreen*, **10** (*3*) 1726–1735 (2023). doi:10.5109/7151721.
25) R. Bhattacharyya, "Dynamics of marine vehicles," John Wiley & Sons, New York, 1978.
26) N.I. Ismail, M.A. Tasin, H. Sharudin, M.H. Basri, S.C. Mat, H. Yusoff, and R.E.M. Nasir, "Computational aerodynamic investigations on wash out twist morphing mav wings," *Evergreen*, **9** (*4*) 1090–1102 (2022). doi:10.5109/6625721.
27) I. Ibinabo, and D.T. Tamunodukobipi, "Determination of the response amplitude operator(s) of an fpso," *Eng.*, **11** (*09*) 541–556 (2019). doi:10.4236/eng.2019.119038.
28) A. Scamardella, and V. Piscopo, "Passenger ship seakeeping optimization by the overall motion sickness incidence," *Ocean Eng.*, **76** 86–97 (2014). doi:10.1016/j.oceaneng.2013.12.005.
29) V.M. Nguyen, M. Jeon, and H.K. Yoon, "Study on the optimal weather routing of a ship considering parametric rolling, slamming and deck wetness," Proceedings of the 13th International Symposium on Practical Design of Ships and Other Floating Structures, Copenhagen, 2016.
30) H. Diatmaja, A.R. Prabowo, N. Muhayat, T. Tuswan, and T. Putranto, "Fast ship prototype design simulation with fin stabilizer on hydrodynamic characteristics for ship realization planning," *IOP Conf. Ser. Earth Environ. Sci.*, **1166** (*1*) 012047 (2023). doi:10.1088/1755-1315/1166/1/012047.
31) A.S. Hadi, and S. Chatterjee, "Sensitivity analysis in linear regression," John Wiley & Sons, New York, 2009.
32) Z. Xu, "On multi-period multi-attribute decision making," *Knowledge-Based Syst.*, **21** (*2*) 164–171 (2008). doi:10.1016/j.knosys.2007.05.007.
33) S.H. Zanakis, A. Solomon, N. Wishart, and S. Dublish, "Multi-attribute decision making: a simulation comparison of select methods," *Eur. J. Oper. Res.*, **107** (*3*) 507–529 (1998). doi:10.1016/S0377-2217(97)00147-1.
34) E. Sugianto, and J.H. Chen, "Hollow wing technique to enhancing conveyor performance on marine debris collection," *Evergreen*, **9** (*4*) 1160–1167 (2022). doi:10.5109/6625727.
35) K. Bhawsinka, "Maneuvering simulation of displacement type ship and planing hull," Memorial University of Newfoundland, 2012.
36) V. Piscopo, and A. Scamardella, "The overall motion sickness incidence applied to catamarans," *Int. J. Nav. Archit. Ocean Eng.*, **7** (*4*) 655–669 (2015). doi:10.1515/ijnaoe-2015-0046.
37) D.P. Sari, T. Tuswan, T. Muttaqie, M. Soetardjo, T.T.P. Murwatono, R. Utina, Y. Yuniati, A.R. Prabowo, and S. Misbahudin, "Critical overview and challenge of representative lng-fuelled ships on potential ghg emission reduction," *Evergreen*, **10** (*3*) 1792–1808 (2023). doi:10.5109/7151729.

38) M. Yusvika, A. Fajri, T. Tuswan, A.R. Prabowo, S. Hadi, I. Yaningsih, T. Muttaqie, and F.B. Laksono, "Numerical prediction of cavitation phenomena on marine vessel: effect of the water environment profile on the propulsion performance," *Open Eng.*, **12** (*1*) 293–312 (2022). doi:10.1515/eng-2022-0034.
39) Seatemparatu.re, "Sea water temperature in kuta (lombok)," (2023). https://www.seatemperatu.re/southeast-asia/lombok/kuta-lombok/ (accessed June 18, 2023).
40) ITTC, "Fresh water and seawater properties - 7.5-02-02-01.02," International Towing Tank Conference, Rio Jenerio, 2011.
41) T. Rahmaji, A.R. Prabowo, N. Muhayat, T. Tuswan, and T. Putranto, "Effect of bilge keel variations on the designed fast patrol boats to hull resistance and stability behaviours," *IOP Conf. Ser. Earth Environ. Sci.*, **1166** (*1*) 012048 (2023). doi:10.1088/1755-1315/1166/1/012048.